Information Sciences Letters
An International Journal

http://dx.doi.org/10.18576/isl/120940

Flood Risk Mapping and Management in Urban Areas: Integrating Geomatics and Hydrodynamic Modeling - A Case Study of Al Bidi City, Saudi Arabia

Ashraf Abdelkarim [1,*] *and Ahmed F. D. Gaber* [2]

[1]Research Center, Ministry of Housing, Riyadh 11461, Saudi Arabia
[2]Department of Geography, Faculty of Art, Sohag University, Sohag 82524, Egypt

Received: 22 May 2023, Revised: 22 Jun. 2023, Accepted: 24 Aug. 2023.
Published online: 1 Sep. 2023.

Abstract: In this paper, we focus on developing a comprehensive approach to map and manage flood risks in Al Bidi City, located in the Al-Aflaj Governorate of Saudi Arabia. By integrating geomatics (Remote Sensing and GIS) and hydrodynamic modeling (PCSWMM and HEC-RAS), the study aims to simulate and model flood risks in populated areas under different scenarios, considering the impact of climate change. The study generates three integrated maps: flood intensity, environmental sensitivity, and flood risks. Strategic solutions and mitigation measures are proposed based on the findings. The results indicate that Al Bidi City is exposed to flood risks originating from the west and progressing towards the east, primarily due to significant valleys such as Wadi Harm. Approximately 60% of the urban area is affected by torrential water. The study proposes the construction of embankments, channels, and culverts to redirect floodwaters to Wadi Al Jadwal in the east, as well as the implementation of industrial channels to manage floods in the northern valleys.

Keywords: Climate Changes; Remote Sensing; Geographical Information Systems; Spatial–Temporal Analysis; Flood Risk Mapping; Environmental Sensitivity Mapping; Flood Intensity Mapping.

1 Introduction

Drainage basins in urban areas in arid and semi-arid environments are exposed to sudden and irregular floods that threaten urban areas and infrastructure. In contrast, the situation becomes more dangerous if the land uses of these basins change [1]. Flood disasters that occur in the dry environment are associated with understanding the geomorphological features of drainage basins and the many processes associated with them [2]. Urban flood risk mapping helps identify areas at risk of potential floods, as well as their hazard according to zoning, which allows decision-makers and planners to manage potential disasters, urban development, and managing urban infrastructure [3]. The damages caused by urban floods of urban areas in the arid and semi-arid environments doubled due to the combined impacts of the increase in extreme precipitation events because of climate change and local heavy precipitation events, with increased spatial and temporal hazard and an increase in peak discharge, runoff and flood events [4,5,6].

Recently, many methods of flood risk mapping have been developed, and perhaps the most prominent and most widely used methods in scientific and practical fields are the (Geomorphometric Ranking Method) [1], as well as the multi-criteria analysis method that is based on geographic information systems (GIS-MCDA) [7]. There is also another standard method in engineering fields for drawing flood risks, which is the risk matrix method that depends on the hydraulic modeling of the two-dimensional program (HEC-RAS) [8,9,10], rate frequency [11,12], the analytical hierarchy method [13], the fuzzy logic [14], logistic regression [15], artificial neural networks [16,17] and the frequency-rate method [18,19]. Undoubtedly, not all of these methods are suitable for modeling flood risks in arid and semi-arid environments in the Kingdom of Saudi Arabia and for determining risks in urban areas.

This study used an integrated approach to integrate geomatics represented by remote sensing (RS) Geographic Information Systems (GIS), and hydrodynamic modeling to have a flood risk map in Al Bidi city and compare it with the recent historical floods that occurred on 18/7/2021. Geomatics represented in remote sensing (RS) and geographic information systems (GIS) provide recurring coverage of flood-prone city areas regularly and rapidly through satellite images and then obtaining temporal and spatial data for floods. In contrast, geographic information systems (GIS) also helped create a distinct work environment with high efficiency and extensive and complex temporal and spatial data.

*Corresponding author e-mail: dr.ashrafgis2020@gmail.com

Undoubtedly, it contributed to the operation and development of the efficiency of hydrological and hydraulic models. This study also relied on hydrodynamic modeling using two-dimensional hydrodynamic models (2D) to calculate flow, their paths, and their impact on populated areas [20,21]. In contrast, the one-dimensional models (1D) are not sufficient to simulate the resulting flow and depths or velocities, while the two-dimensional modeling (2D) more accessible, easier, and more widely used with the increasing computational power [10,22], the quality of geographic information systems-based data and the availability of digital information with survey mylar data; thus the two-dimensional modeling is a solution to assess flood problems in populated areas [9]. At this stage, the well-known two-dimensional modeling program was used (PCSWMM (2D)); which is a hydrodynamic model developed by (Computational Hydraulics International (CHI)) that can make hydrodynamic models (1D-2D) for stormwater drainage networks, open channels, culverts, bridges, dams, analyzing drainage basins, and making hydrological models of surface flows, in addition to determining the sanctuaries of valleys and areas exposed to the dangers of torrential rains and rainwater gatherings [23,24].

The PCSWMM (2D) program is considered one of the best and highest rated models in the field of hydrodynamic modeling, especially about its complexity, ease of use, degree of simulation, and providing detailed results in good presentation [25,26]. This was all done by relying on the comparison between the results of the (PCSWMM (2D)) program and the results of the two-dimensional hydraulic modeling program (HEC-RAS). Floods have significantly increased since 2005 in the Kingdom of Saudi Arabia due to locally heavy rains and geographical conditions, as most regions and cities were exposed to hefty rains within a short period, which makes these rains sudden, rapid and unpredictable, in addition to the low capacity of soil absorption of water, which leads to an increase in the flow of water, urban expansions, change in the map of land uses, and continuous and unjust construction in the valleys, which has increased the incidence of casualties and damage in many cities of the Kingdom, including Al Bidi city.

The study dilemma is summarized in: (1) that the city of Al Bidi is exposed to many recurring torrents, the last of which is the torrents that occurred on 18/7/2021, as a result of attacking many valleys coming from the west, the most important of which are Wadi Harm, Shaib Ab Ash Darr, Wadi Al Hinu, and Wadi Al Jadwal, which led to severe damages from cutting off main roads and some secondary roads. The sinking of many buildings Figure **(1)**, **(2)** Deterioration of the map of land use. The emergence of environmental problems as a result of the inability to drain rainwater and torrents **, (3)** Inability of culverts existing under Ar-Riyadh -Wadi Ad Dawasir road to contain the passing flow, and some of them were blocked due to the remnants of torrents during their flow while being unable to drain the incoming floods in abundance, **(4)** Drop in the level of the Ar-Riyadh - Wadi Ad Dawasir road when it passes through Wadi Harm, which led to its easy flooding, causing significant damage to a number of vehicles and stopping the movement of passengers, **(5)** the absence of using appropriate hydrological and hydraulic models for evaluating and producing flood risk maps in the Arab city. The flood risk map in Al Bidi city presents the spatial extent of floods with different scenarios and compares them with the recent historical floods that occurred on 18/7/2021.

The purpose of this study is to model, simulate, evaluate and manage the flood risk map in Al Bidi city as a model for the Arabian city, which is exposed to frequent flood risks based on the approach of integrating geomatics and hydrodynamic modeling. This approach is more distinguished in terms of its applicability in urban areas. In contrast, this approach includes developing water depth maps and maps of flood velocity and hazard. A methodology will be presented to assess the extent of the danger of floods resulting from valleys in the study areas represented in various facilities and different land uses, as this risk varies from one place to another. The different degrees of risks were clarified relative to each other, taking into account the severity of the flood and the degrees of sensitivity of the areas exposed to such risk by converting the numerical data deduced from hydraulic models into analytical maps.

Source: https://sabq.org/saudia/nhgrh9

Fig. 1: The impact of the historical floods that occurred in the city of Al Bidi, including (a) cutting, destroying, and stopping the road of Wadi Ad Dawasir - Al Bidi, (b) the floods of Wadi Harm on the neighborhoods of Al Bidi city on

18/7/2021

2 Materials and Methods:

2.1. Study area:

Al Bidi city is located in Al-Aflaj Governorate, around 300 km south of Ar-Riyadh, Kingdom of Saudi Arabia. It is about 38 km from Layla city, and its urban area is approximately 70 km². In contrast, it includes in its formation Al Bidi Ash Shamali and Al Bidi Al Janubi, with some planned and old neighborhoods. As for the geographic location, it is located between the latitudes 22° 4' 47.15" and 21° 58' 56.67" North, and the longitudes 46° 37' 42.41" and 46° 31' 27.09 East. Al Bidi used to be called in the old times Al-Mathare', whereas Al-Mathare' is the plural of Al-Madhra'a, the middle country between the countryside and the land. The city of Al Bidi is affected by a group of valleys coming from the west, which leads to the sinking of the main road that penetrates the city and most of the city's neighborhoods. The city is located in the flood plain area of weak slopes, and that is why the water coming from the flood's spreads in the horizontal direction in a more significant way than usual, as the study area is located within a flat/flat topography that makes the flow disperse without recognizing a clear path thereof**.** (Figures 2 and 3).

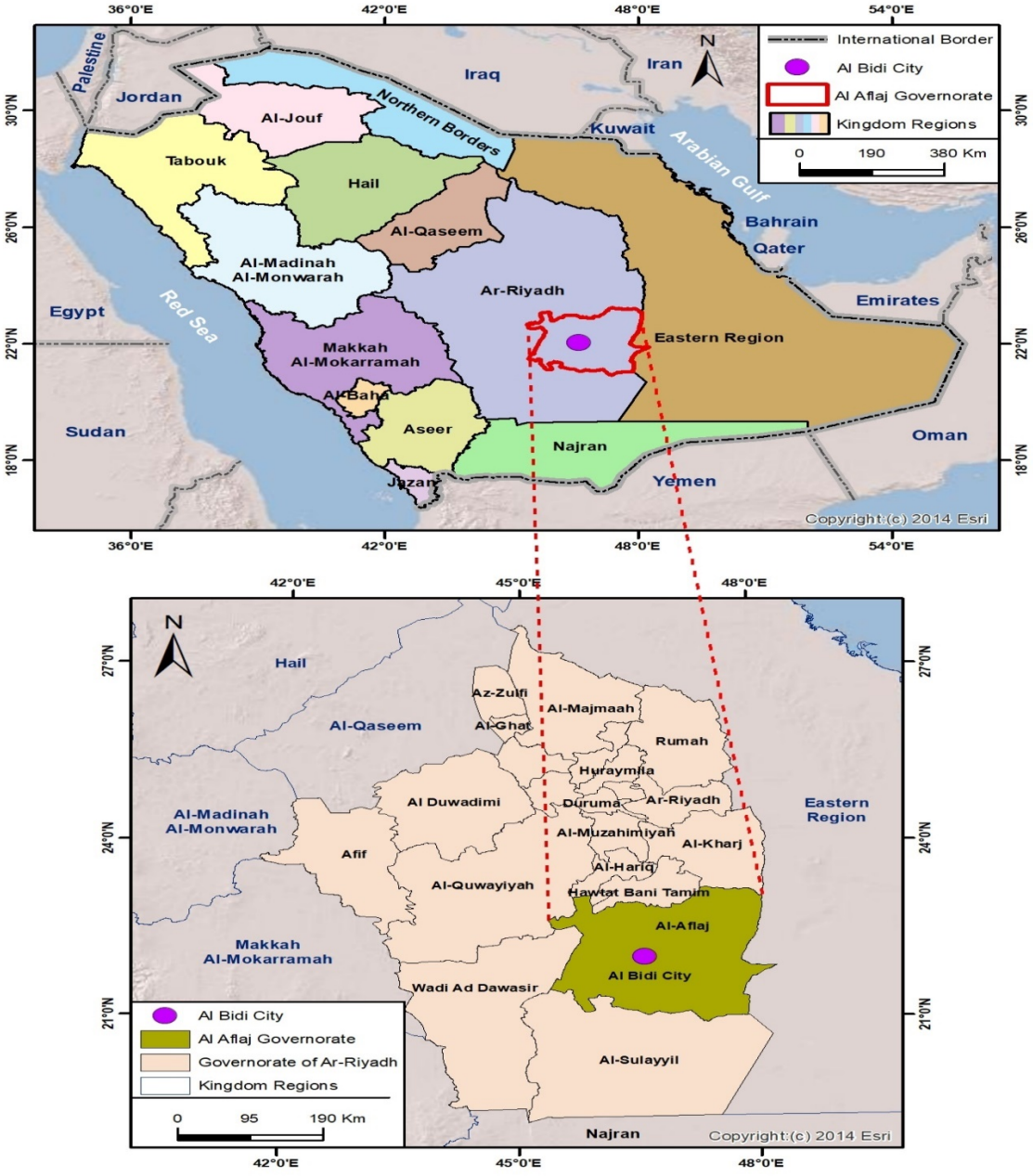

Fig. 2: The location of the study area from Al-Aflaj Governorate and the Kingdom of Saudi Arabia

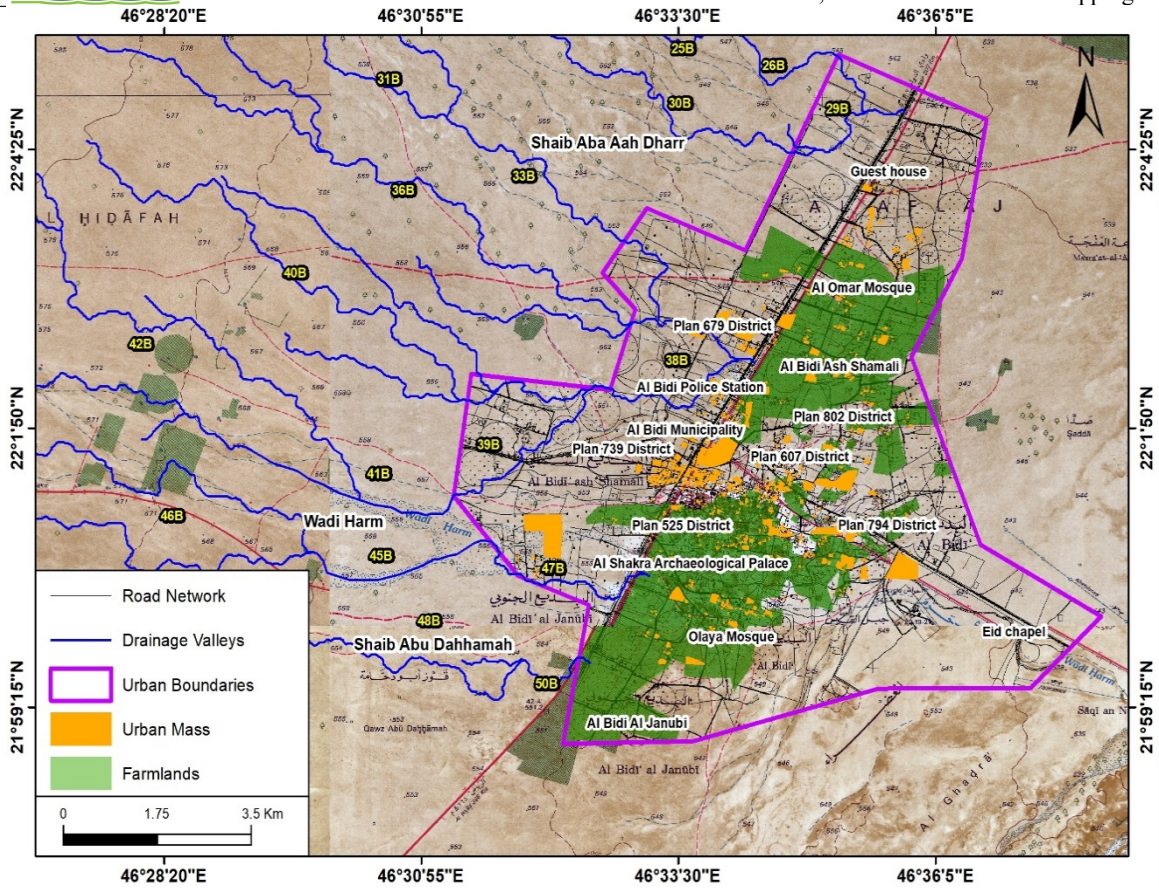

Fig. 3: The network of valleys affecting the city of Al Bidi from the topographic map of the Saudi Geological Survey at a scale of 1:50,000

2.2. Identifying Data Sources:

Several sources of spatial data were used in this study, as satellite image data and lidar data were used to monitor the recent historical floods that the city was exposed to, and many other digital maps were integrated, such as: Topographic maps, Geological maps, and Rain stations data, Table (1) indicates the collected data used to complete the study and presents its characteristics, including spatial accuracy and sources.

Table 1: Input data, spatial clarity and their sources used in the study

Layers	**Data used to extract the layers**		**Entities/locations used to obtain the data**
	Source	**Scale/spatial accuracy**	
Valleys	LiDAR Data	50 cm	Ministry of Municipal and Rural Affairs and Housing
	Topographic maps	1:50,000	Saudi Geological Survey
Land use	Satellite image Landsat 8	30m	http://earthexplorer.usgs.gov
Rain stations	Al Bidi (SU101) and Al-Hadar (SU102)		Ministry of Environment, Water and Agriculture
Geological formations	Geological maps	1:500,000	Saudi Geological Survey
Soil Hydrological Group			
Flood water drainage facilities (culverts, Embankments, Tranquilization Lake)	Survey Work		Ar-Riyadh Municipality
	The researcher's field study		Visit the study area
Basemap and various services	1:5,000		Surveying works, Municipality Secretariat for the districts

Layers	**Data used to extract the layers**		**Entities/locations used to obtain the data**
	Source	**Scale/spatial accuracy**	
Administrative borders of the Kingdom of Saudi Arabia and the governorates	1:5,000		Official Map, Geospatial Portal, General Survey Authority, and Atlas of Maps of Distributions of the General Population and Housing Census Results, General Statistics Authority

2.3. Methodology:

Figure (4) illustrates the methodology and study procedures used to determine the flood risk map in Al Bidi city, which depends on integrating geomatics and hydrodynamic modeling through the production of three digital maps, which are the flood intensity, environmental sensitivity, and flood risks maps. The data processing steps can be traced as follows.

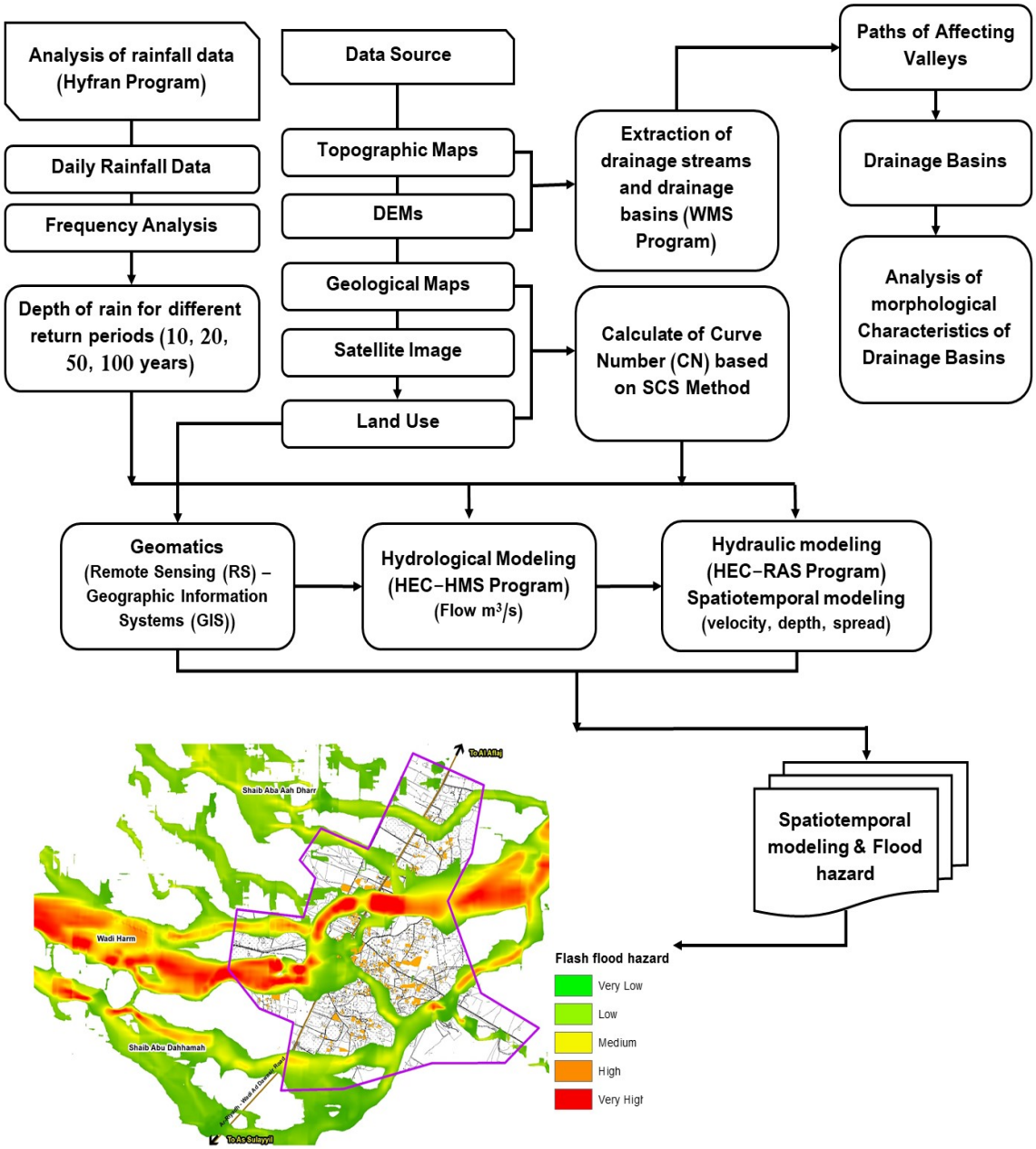

Fig. 4: Study methodology and procedures

2.3.1. Hydrological Modeling:

2.3.1.1. Calculate lag time and time of concentration using the SCS method:

The primary factor WMS provides several hydrological models, the most important of which are TR-55, HEC-1 and HEC-HMS. Each model provides equations for calculating Time of Concentration and Lag Time. It should be noted that choosing the appropriate model is very important in hydrological modeling, as this choice is related to methods of calculating Time of Concentration, Lag Time, losses and hydrographs. For example, when choosing the hydrological model HEC- 1, the program will provide key, popular ways in which to calculate Time of Concentration and Lag Time, such as the Clark method (UC), the Snyder method (US), and the method for managing soil conservation services (SCS dimensionless UD), and the given (observed) unitary water curve method (Given unit Hydrograph UI), and the kinematic waves (UK) method. Each method provides equations for calculating Time of Concentration and Lag Time. In this study, the most important were calculations available within the hydrological modeling were used. For example, the Kirpich equation was used to calculate Time of Concentration, which is the time needed for rainwater falling on surfaces of basins to gather until the point where the level of flow needs to be calculated [27]. This is done using equation (1):

$$t_c = 0.0195\left(\frac{L^{0.77}}{S^{0.385}}\right) \quad (1)$$

Where: Tc = Concentration time (min), L = Critical path length for water (km), S = basin surface slope (%).

The Lag Time was calculated using the SCS Method equation which is the time that elapses between the occurrence of a unit of rain and the occurrence of a unit of flow [28], by equation (2):

$$T_{LAG} = \frac{L^{0.8}[Sr+1]^{0.7}}{1900\sqrt{Y}} \quad (2)$$

Where: T_{LAG} = lag time (hours), L = Longest path of water (feet), Sr = Maximum soil moisture potential (Maximum retention) and is calculated from the curve coefficient, Y = General slope of the basin (%).

2.3.1.2. Calculation of the effective rain intensity (flood) using curve number:

The intensity of the rain or direct flood in the basin was calculated to infer the total amount of floods at the actual rain value through equations (3-5), and the amount of water in the area was estimated before the occurrence of the flood such as infiltration and rain suspended on the plant using the equation (3). Equation (4) can be simplified as shown in equation (5) [29]:

$$Q = (P - Ia)^2/(P - Ia + S) \quad (3)$$

$$Ia = 0.2Sr \quad (4)$$

$$Q = (P - 0.2Sr)^2/(P + 0.8Sr) \quad (5)$$

Where: Q = Direct flow (cm), P= Rain for different frequency periods (cm), Sr = Maximum soil moisture potential, Ia = The amount of water before the flood, such as infiltration and rain suspended on plants.

The maximum soil moisture potential is calculated as CN represents CN using the Soil conservation services (SCS) method, and this parameter depends on the nature of the soil and land use using equation (6) [29]:

$$S = (1000/CN) - 10 \quad (6)$$

2.3.1.3. Calculating the maximum discharge for each basin:

The greatest discharge (m^3/s) for each basin for different iterative periods, using equation (7) [29]:

$$qp = \frac{0.208AQ}{Tp} \quad (7)$$

Where: qp = greater discharge (m^3/s), A= Area in square kilometers, Tp = Time to maximum discharge (m^3/s), Q= the amount of surface runoff (mm), and the time to maximum discharge is calculated using the following equation (8) [29]:

$$Tp = \Delta t/2 + TL \quad (8)$$

Where: Tp = Time to peak flow (hours), Δt = Design Storm duration, TL = Lag Time (hours).

There are five methods of channel routing in (HEC- HMS) [30], two of them have been used here:

(1) The Muskingum directive method uses a simple estimation of the finite difference to solve the following equation

$$O_t = \left(\frac{\Delta t - 2KK}{2K(1-X)+\Delta t}\right) I_t + \left(\frac{\Delta t - 2KK}{2K(1-X)+\Delta t}\right) I_{t-1} + \left(\frac{2K(1-X)+\Delta t}{2K(1-X)+\Delta t}\right) O_{t-1} \quad (9)$$

Whereas:

O = is the outflow

I = is the inflow

t = time and K and X are parameters that depend on the channel and flow characteristics.

(2) The modified pulse method, also known as storage routing or plane pool routing method, is based on the approximation of the finite differences of the continuity equation and is coupled with an empirical representation of the momentum equation. The regular expression is given by

$$\left(\frac{S_t}{\Delta t} + \frac{O_t}{2}\right) = \left(\frac{I_{t-1}+I_t}{2}\right) + \left(\frac{S_{t-1}}{\Delta t} + \frac{O_{t-1}}{2}\right) \quad (10)$$

Whereas

I and O are the inflow and outflow, S is the storage in the channel access, and t is the time. A functional relationship between the storage and the outflow is required to solve this equation [31].

2.3.2. Hydraulic Modeling:

The risk assessment process in this study is based on an integrated approach between geomatics and hydrodynamic modeling and depends on the production of three types of maps, namely:

- Flood intensity map.
- Environmental sensitivity map.
- Flood risks map.

2.3.2.1. Flood intensity map:

Flood intensity maps are defined as maps showing the geographical distribution of flood intensity with different degrees. The depth and speed of the flood resulting from two-dimensional hydraulic modeling are considered. At first, the geographical distribution of flood depth and velocity is deduced from the results of two-dimensional hydraulic modeling. This distribution is the depth, and velocity values deduced from hydraulic modeling. Maps of water depth, speed, levels, and flood intensity have been created, and by using the energy conservation equation, it is possible to calculate the velocity and depth of water [32,33,34]. Several previous studies have shown that these models have resulted in accurate and effective flood studies [35,36]. The flood intensity is then rated according to the equation DEFRA [21,22,37].

$$HR = D * (V + 0.5) + DF \quad (11)$$

Whereas:

HR: Flood intensity rating

D: is the water depth (m)

V: is the water velocity (m/sec)

DF: debris coefficient.

The debris coefficient is calculated in Table 2.

Table 2: Determination of the debris coefficient (Rubble Coefficient)

Debris coefficient (DF)	depths (m)
0.5	**0 to 0.25**
1	**0.25 to 0.75**
1	**greater than 0.75 or velocity greater than 2 m/s**

After calculating the rating value, the flood intensity is arranged according to Table 3.

Table 3: rating of flood intensity

Risk rating	Flood intensity value
There is no risk	0
low risk	<0.75

medium risk	0.75-1.25
severe risk	1.25-2.0
maximum risk	>2.0

2.3.2.2. Environmental sensitivity map:

They are maps showing the degree of vulnerability or impact of the study areas on floods. Land uses that express the degree of area's importance and sensitivity are rated from 1 to 5 according to the degree of flood vulnerability. Priority is given to residential and governmental sites, public services, and utilities, while the priority is lowered to desert and remote areas. Flood impact assessment is a critical component of flood risk management strategies, and flood vulnerability mapping is valuable as it helps in spatial visualization where vulnerabilities are low or high [38,39], and Table 4 indicates the values of the degree of sensitivity to floods.

Table 4: The degree of land affected by torrential rains according to the type of use

Type of use	Flood vulnerability
residential	5
governmental	5
utilities	5
amenities	5
Airport	5
Parks	2
Agricultural areas	1
Desert areas	0

2.3.2.3. Flood Risk Map:

They are maps showing the areas exposed to the risks resulting from floods with different degrees of these risks relative to the geographical distribution. These maps are calculated by taking into account the severity of the flood and the degree of sensitivity of the area to this flood. Flood risk maps can be used as an effective tool for water resources and urban planning by design engineers to assess the exposure of infrastructure and residents in this area to flooding [40]. Flood risk maps and risk analysis for any of the drainage basins include several factors or criteria [41,42].

2.3.3. Verify the accuracy of hydrological and hydraulic modeling:

Modeling is a simulation of natural phenomena as much as possible so that we can later anticipate different scenarios and develop possible solutions. Any model depends primarily on three basic elements:

Inputs: are the data that are analyzed using the equations that the model calculates, noting that these data are not changed because they were measured from nature or deduced from other accounts.

Outputs: are the results deduced from calculating the equations carried out by the model, whose values are compared with the existing values in nature, in order to verify the accuracy of the model.

Coefficients: are values that express the nature of the area, which are changed if the outputs are not equivalent to the nature values, until the results are consistent and modeling accuracy is ensured, and the conformity of the outputs is verified according to the following Root Mean Square Error equation [43]:

$$\mathrm{RMSE} = \sqrt{\frac{\sum_{n=1}^{N}(\hat{r}_n - r_n)^2}{N}} \quad (12)$$

Where $\hat{r}_n$ means the prediction rating; r_n means the true rating in testing data set; N is the number of rating prediction pairs between the testing data and prediction result.

During this phase of the project, verification of the 2D Hydraulic Model HEC-RAS was carried out using the 2D Hydraulic Model PCSWMM.

3. Results:

3.1. Geometric Morphometric Characteristics:

The drainage basins affecting Al Bidi city were divided using LiDAR Data with the accuracy of (50 cm), whereas the high-resolution LiDAR Data is considered one of the main factors in flood risk modeling studies [44,45]. The drainage basins affecting the borders of Al Bidi city were identified, and the drainage basins involving the existing culverts were divided, to evaluate the facilities to prevent the risks of floods according to the quantities of water descending on them,

while internal drainage basins (within population centers and gatherings) were divided when assessing the current situation, to determine the quantities of water flowing into each element of the existing flood risk prevention facilities for hydraulic evaluation and recommendations, Figure (5).

Figure (6) illustrates the topography of the basins of the study area. Al Bidi city consists of flat plains, medium-rise mountains, and valleys. The site rises about 559 meters above sea level, and the land slope in the Al Bidi area descends from west to east. Al Bidi city passes several valleys, the most important of which are Wadi Harm, the Al Bidi Ash Shamali valley, and the Al Bidi Al Janubi valley. In contrast, each of them descends from the west to the east, in addition to the branching streams. Some fertile plains with abundant water are suitable for cultivation near the Al Bidi Ash Shamali Valley. There are some regional heights, such as Jibal Tuwayq near Wadi Harm. In contrast, it rises by around 559 meters above sea level. But most of its slopes are flat and oriented towards Wadi Harm.

3.2. The maximum amount of daily rain and the determination of the depth of rain for different frequency periods:

The report on climate condition expectations in 2050 in the Kingdom of Saudi Arabia was considered, which presented seven climate models. The scenario (RCP 8.5) was adopted, whereas the annual average was 112 mm; this scenario gives the highest rate of change in the expected rain expected rate in 2050, which amounts to 19% of the predicted rainfall rate. The impact of this percentage on the frequent storm of 100 years has been calculated.

Two meteorological stations were relied upon: Al Bidi (SU101) and Al Hadaar (SU102), affiliated to the Ministry of Environment, Water and Agriculture, as they are the closest rain gauge stations to the study area, and because of the presence of more than one rain station affecting the drainage basins. Theissen Polygons were created to recognize the impact of each station on the basis of the study area. The Theissen Polygons method is based on the principle of linking the extent of the impact of each rain station with the area of the land of the drainage basins affected by this station, and the method depends on drawing polygons that divide the basin land into parts, each of which falls under the direct influence of one monitoring station.

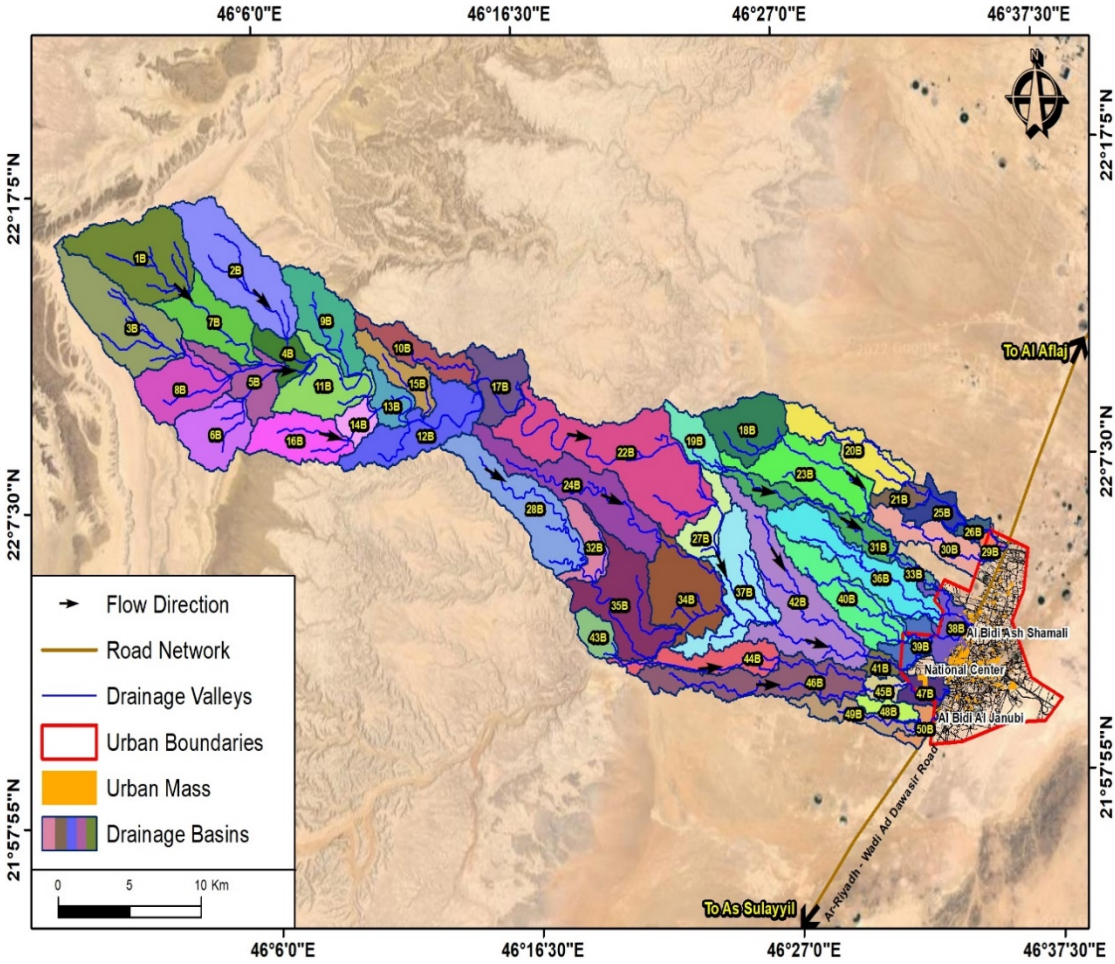

Fig. 5: The drainage basins and the valley network affecting the study area

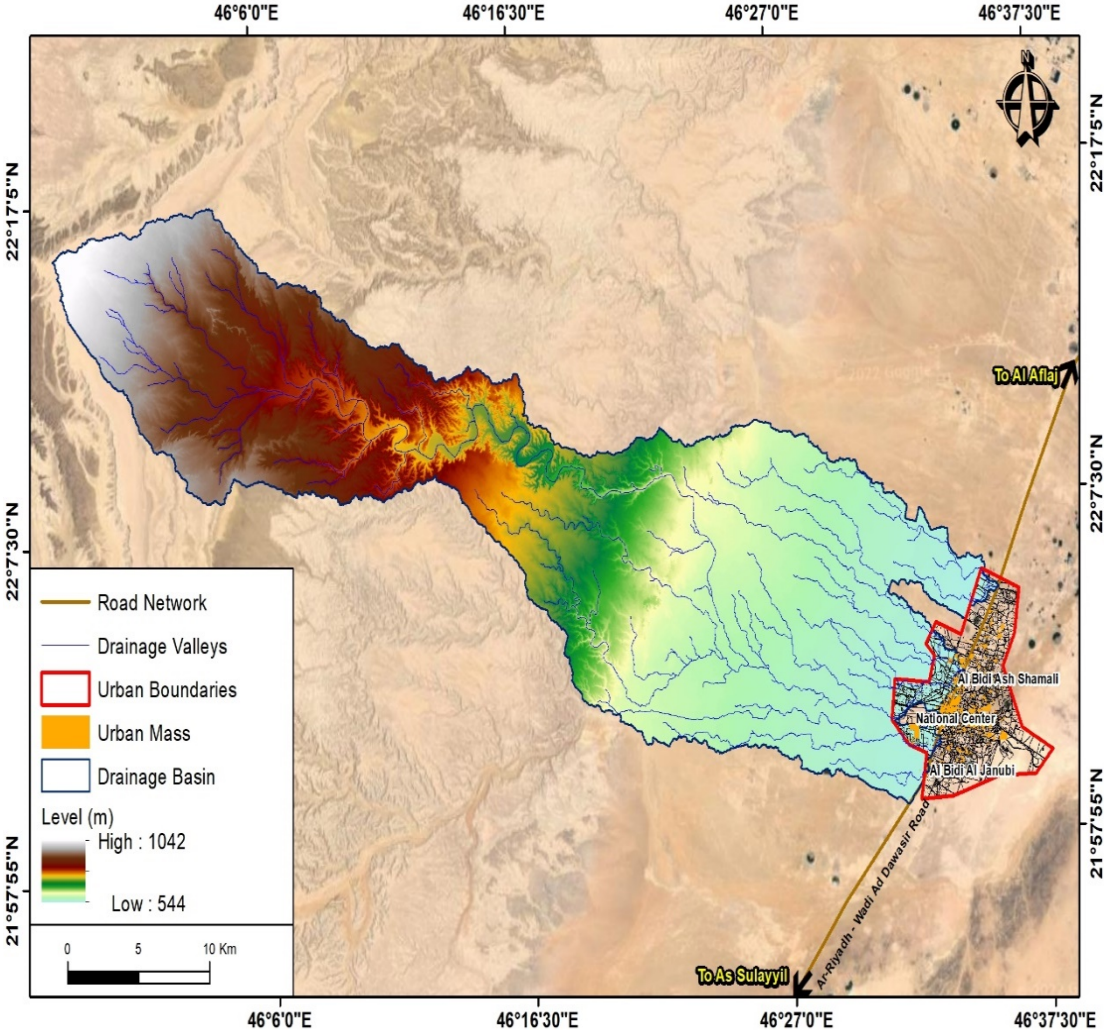

Fig. 6: Topography of the study area basins

The values of rain depth for the recurring periods (10, 20, 50, 100 years) were extracted from Table No. (5) and Figure No. (7), using the statistical analysis program Hyfran, and the application of various statistical distributions, such as the method: Gamma , and Gumbel , andParameter-3, and Pearson Type III, and Log-Pearson Type III, and Exponential, and Normal, and Lognormal, and GEV, and Weibull.

Table 5: Rain stations affecting the study area

Station code	Station name	east coordinate	North coordinate
SU102	Al Hadaar	45.95	21.99
SU101	Al Bidi	46.55	22.019

3.2.1. Equivalent Depth of Rainfall (Equivalent Rainfall):

Shown below is the average rainfall equivalent to the drainage basins affecting the city of Al Bidi, with a total area of 738.63 km^2, Table no. (6 and 7).

Table 6: The impact area of each station on the drainage basins

Station	The area of the basin inside the influencing station (km^2)	Total basin area (km^2)
Al Bidi (SU101)	447.74	738.63
Al Hadaar (SU102)	290.89	

Table 7: Equivalent Depth of Precipitation (Equivalent Rainfall) for drainage basins

recurring periods	10	20	50	100
Equivalent precipitation depth (mm)	54.99	63.88	74.56	81.93

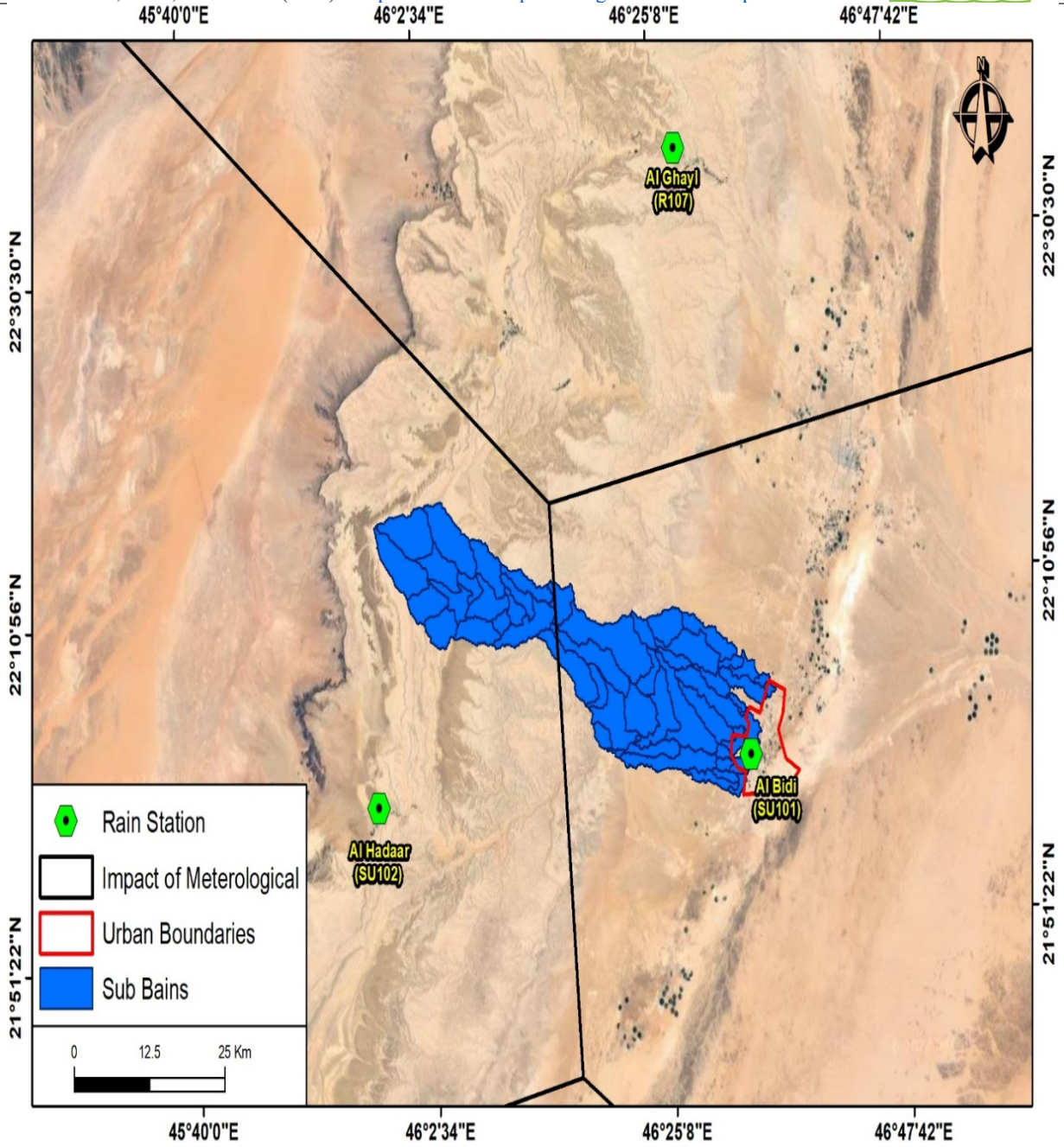

Fig. 7: Rain monitoring stations and drainage basins affecting the study area

3.3. Soil Hydrological Group and Curve No.:

The city of Al Bidi is located within the geological map of the Southern Tuwaiq Square No. (I-212A), at a scale of 1:500,000, and it was found that the soil on the west side is of type (Type A), and this type of soil is characterized by being cohesive soil, and soils are often (Type A): Clay, loam, sandy loam, alluvial loam, and in most cases it is clay, alluvial loam, and sandy loam, while the eastern part soil is of the type (Type B) such as gravelly loam and clay loam. Figure No. (8) indicates the geological map of the drainage basins affecting the study area, while figure No. (9) indicates the hydrological group of the soil of the drainage basins affecting the study area. As a result of the mud structures of the valleys' sources; the values of their curve number range from 70 to 86, which increases the amount of runoff surface and flow rate of rainwater and torrential valleys and branches of which the paths penetrate the urban communities in the city of Al Bidi. The curve number values range from 75 to 76 to the west of the study area, where the high-permeability areas are located, while the curve number values for the areas adjacent to the study area were considered from 76 to 86, Figure No. (10).

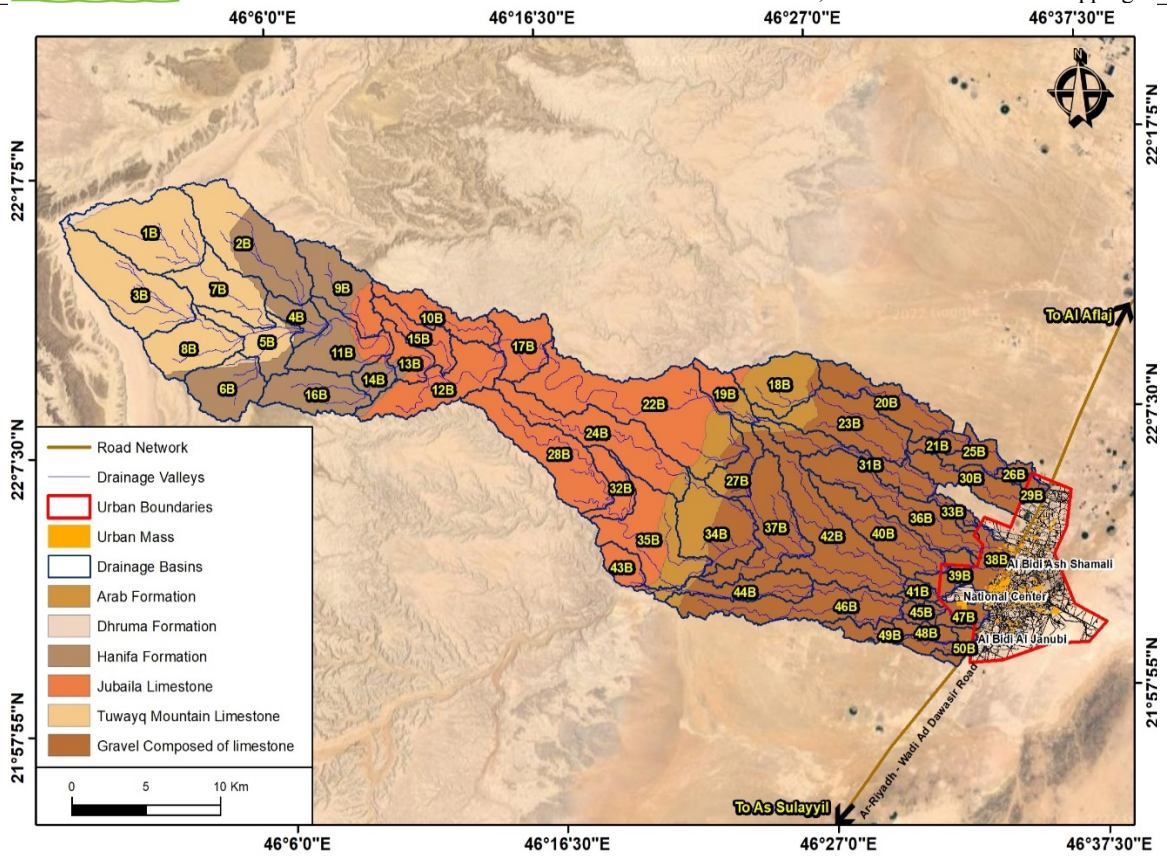

Fig. 8: Geological map of the drainage basins affecting the study area

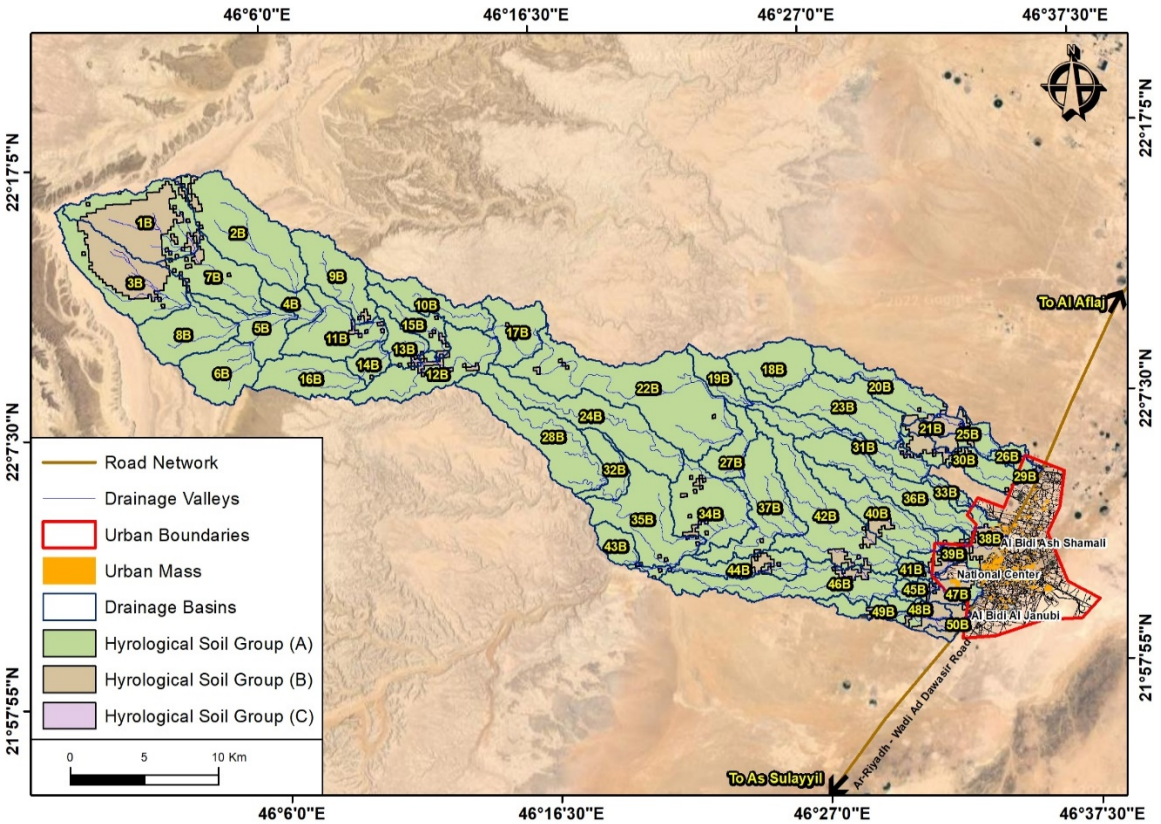

Fig. 9: Soil Hydrological Group of Drainage Basins Affecting the Study Area

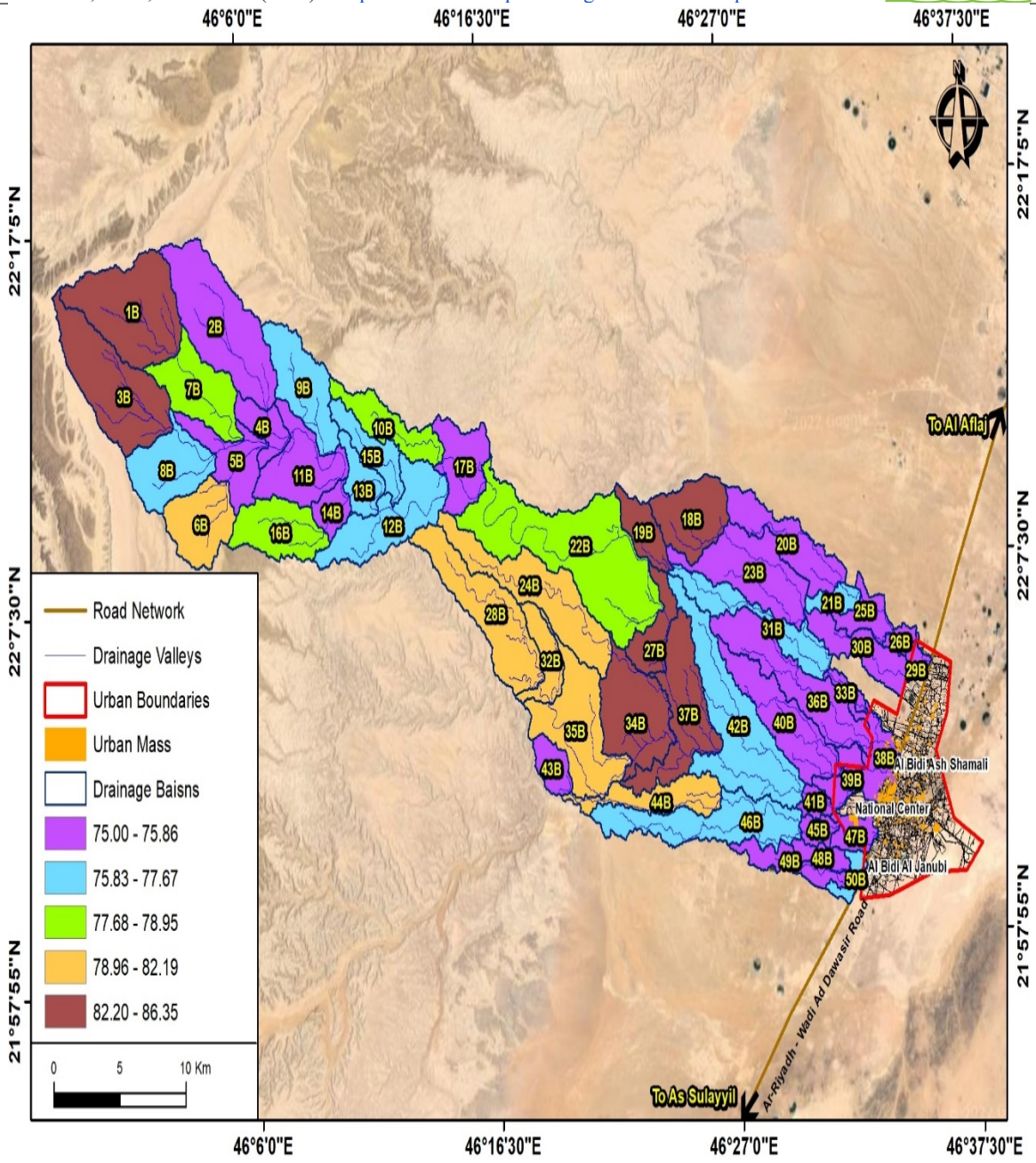

Fig. 10: Curve Number of Drainage Basins Affecting the Study Area

3.4. Characteristics of torrential water:

The flow values of the drainage basins affecting Al Bidi city ranged between 1.50 m^3/sec and 170 m^3/sec. Figures (11:16) show the total drainage points deduced from the drainage basins with the corresponding hydrograph for each point. Table no. (8) indicates the maximum behavior values for each Hydrograph.

Table 8: Maximum drainage point flows

drainage point	The maximum value of the discharge (m^3/sec)
79C	4.1
83C	16.6
86C	2.3
88C	170
97C	7.0
99C	1.50

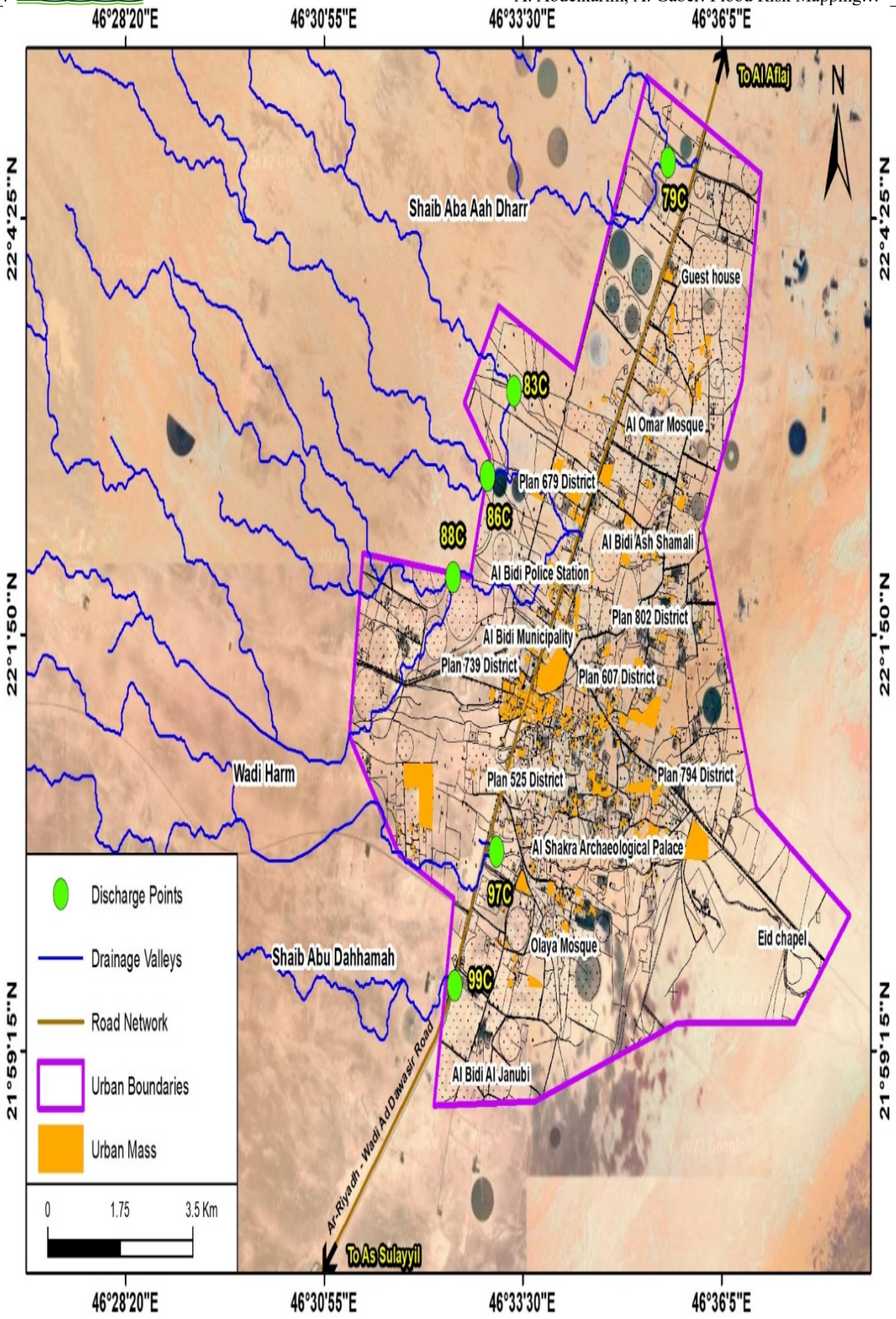

Fig. 11: Drainage points affecting the study area

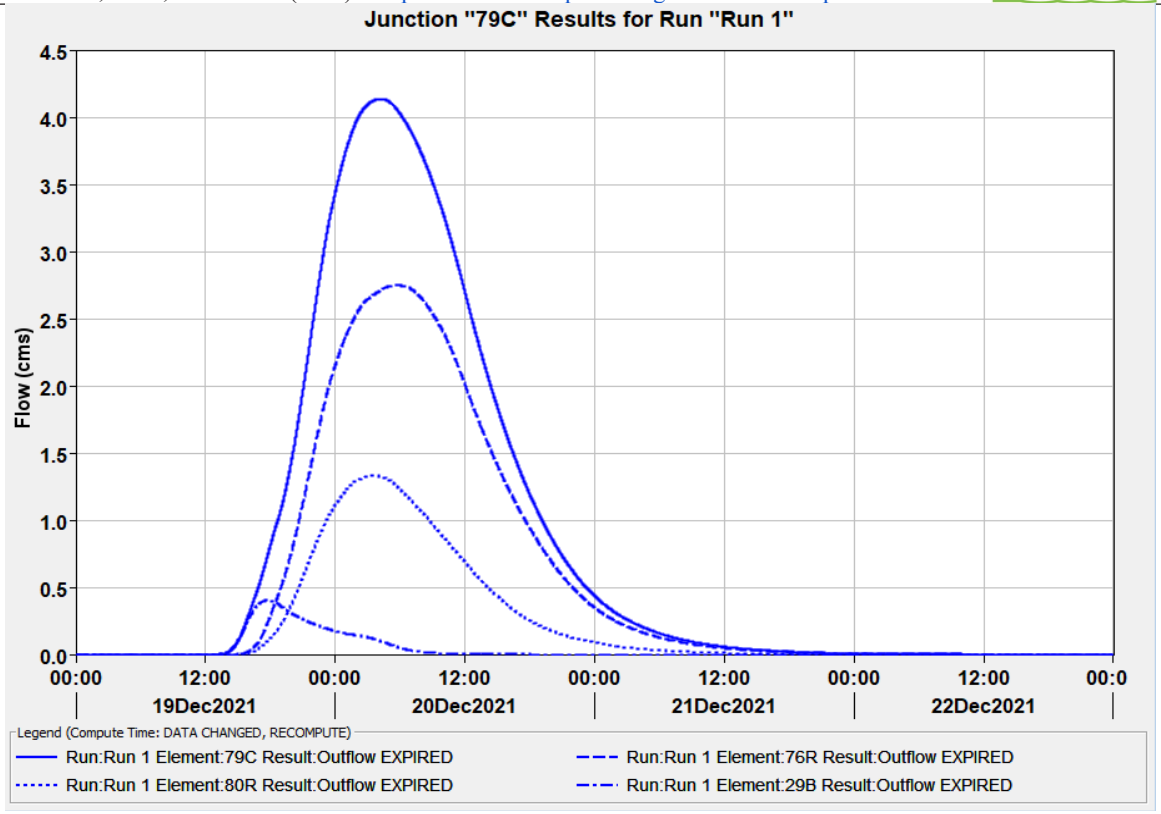

Fig. 12: Hydrograph of the drainage point 79C

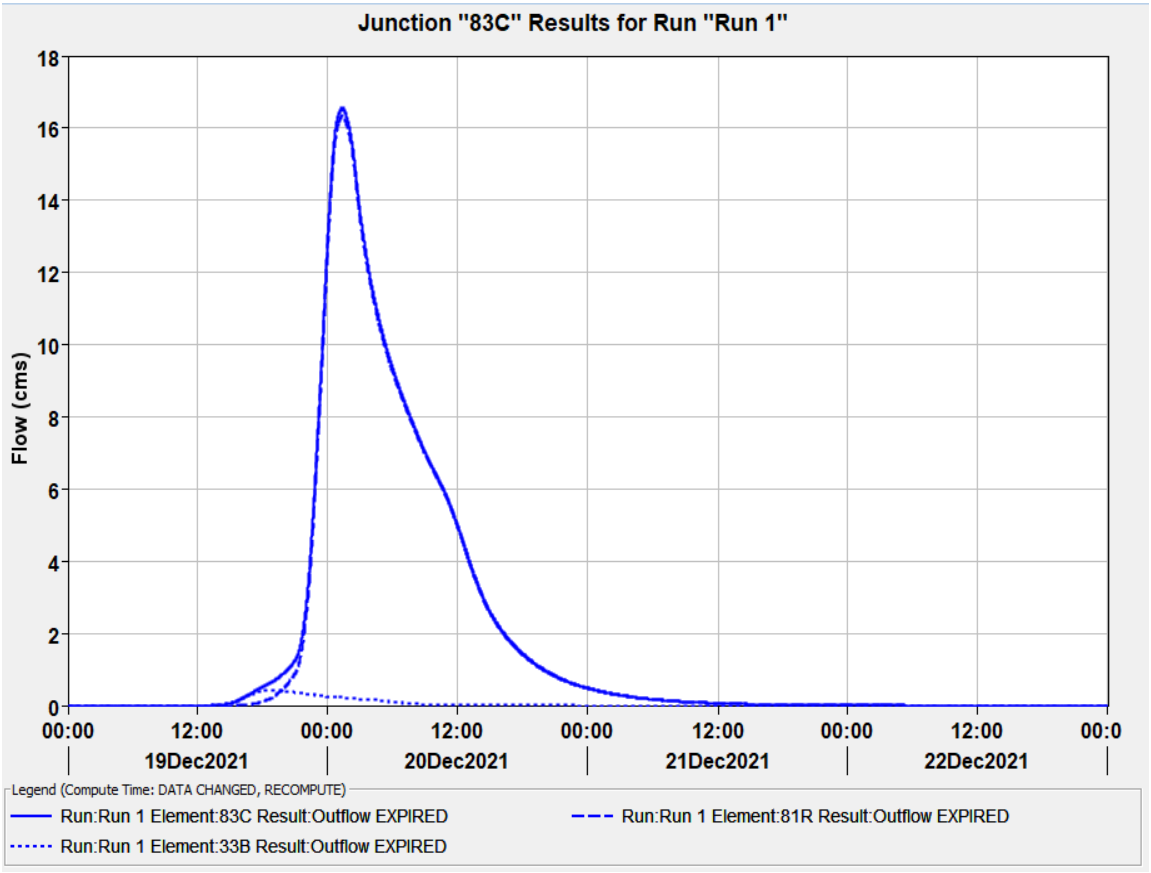

Fig. 13: the hydrograph of the drainage point 83C

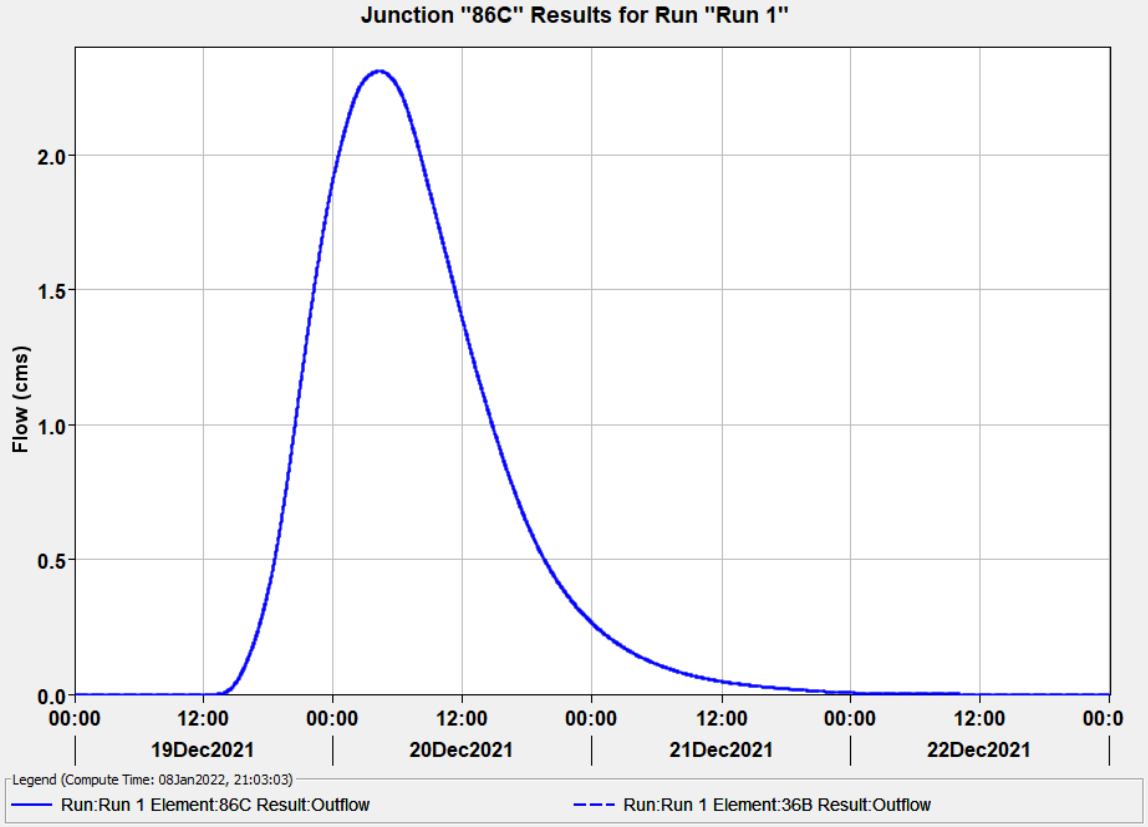

Fig. 14: Hydrograph of the drainage point 86C

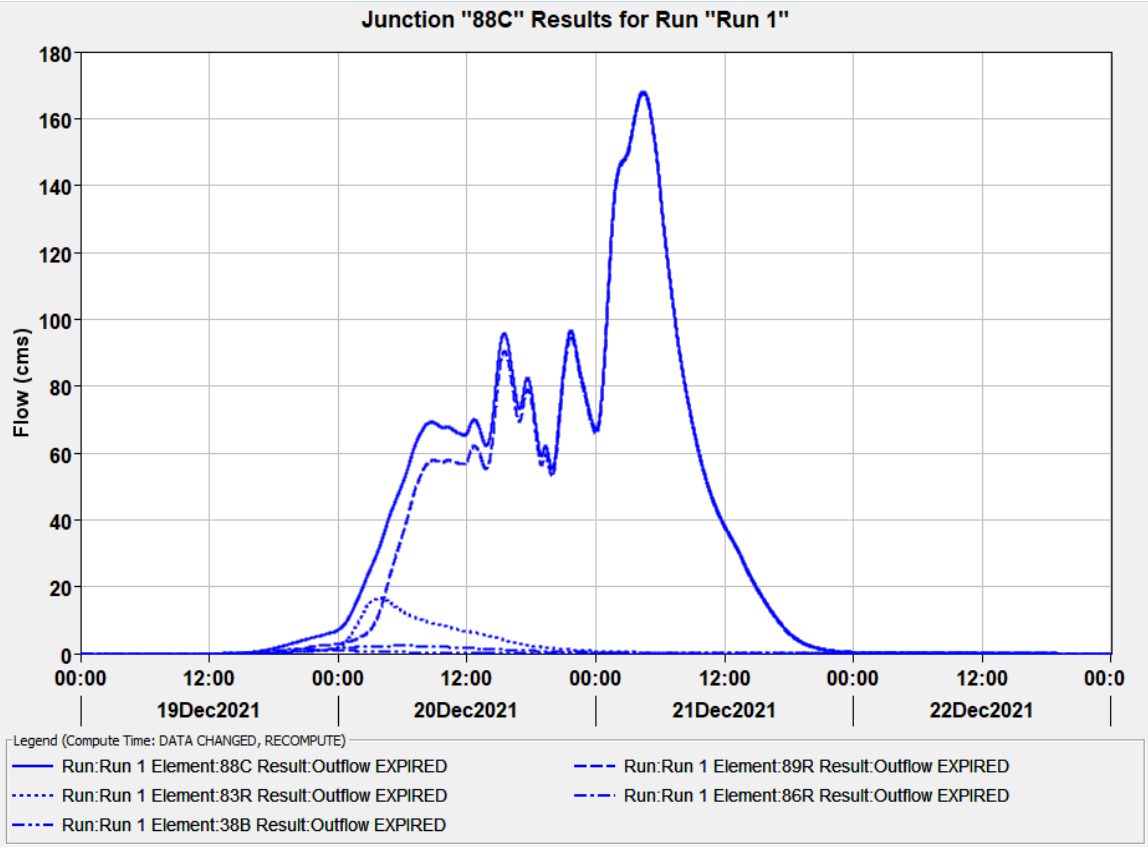

Fig. 15: Hydrograph of the drainage point 88C

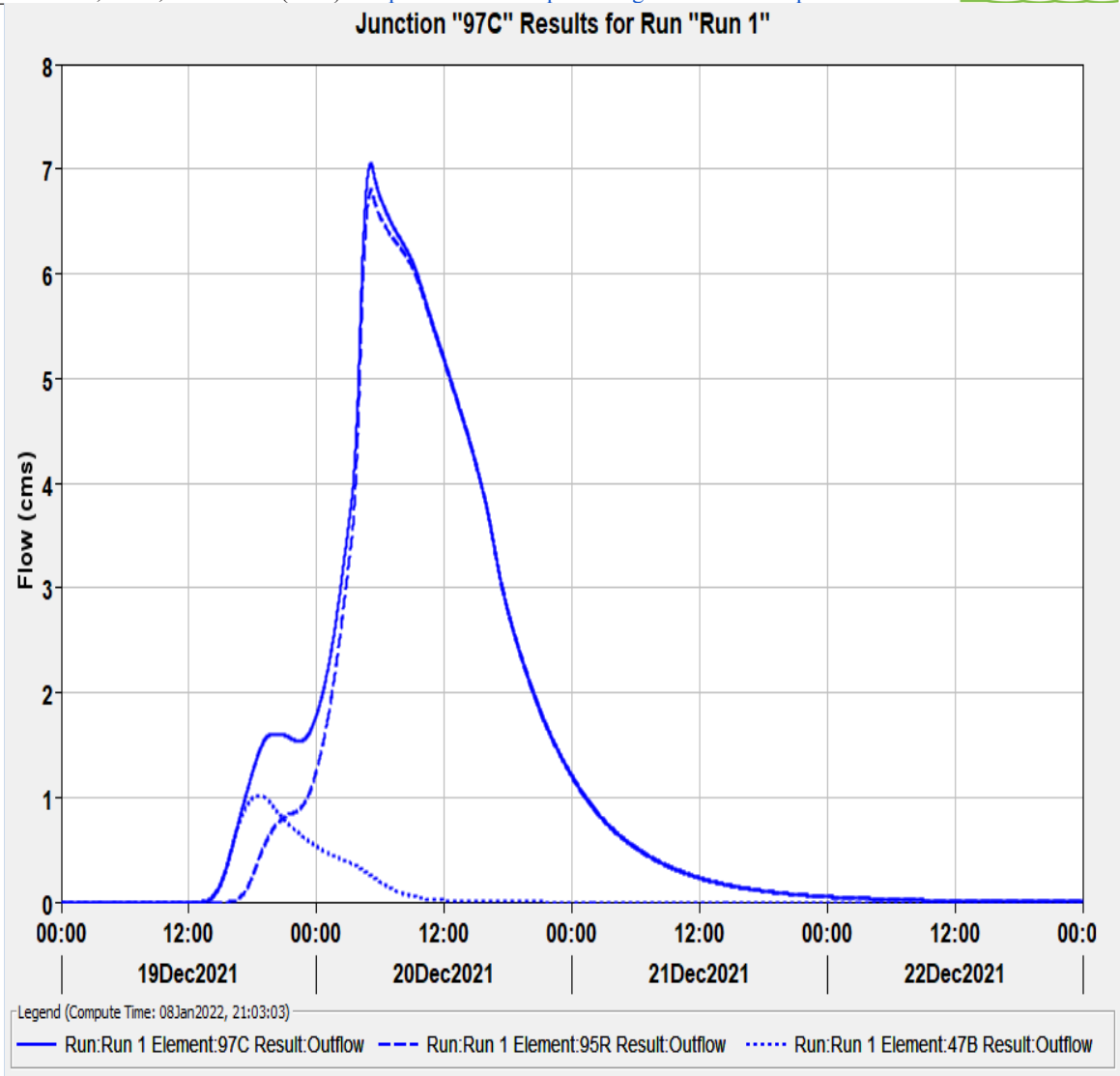

Fig. 16: Hydrograph of the drainage point 97C

3.5. Analysis of 2D Modeling Characteristics (Depths (m) – Velocities (m/s)):

This stage depends on the presentation of the two-dimensional modeling results (two-dimensional modeling), whereas a modeling of the current and future situation was done (after proposing solutions) using the two-dimensional program (HEC-RAS), and in order for the program to model, it must be given the appropriate coefficient of friction for each area, while Figures (17,18) show the results of depth and velocity from the modeling of the existing situation, and the results of the two-dimensional hydraulic modeling showed (two-dimensional modeling) that the maximum speed reaches 1.2 m/s, and that the maximum depth reaches 2.2 m during the 100-year storm. These depths and velocities are concentrated in the neighborhoods of the scheme 739, 679 and 525 and in the Al Bidi municipality area, and the National Center, which are the downtown areas and are mainly affected by the torrential rains of Wadi Harm. This is due to the noticeable flatness of the earth's slopes, which leads to a decrease in water velocity and its accumulation in different places. The areas at risk have been verified and it was ensured that they are exposed to drowning through the available videos and images of the various storms of the city, as well as modelling the future situation after proposing appropriate solutions, which will be clarified in detail in the proposed situation part.

3.6. Validation of the Flood risk Model:

The areas at risk were verified and ensured that they were subject to drowning through the available videos and photos of different storms and a field visit to the city, Figure No. (19), in addition to modelling the future situation after proposing appropriate solutions, which were explained in detail in the protection and prevention plan to ward off the risks of floods.

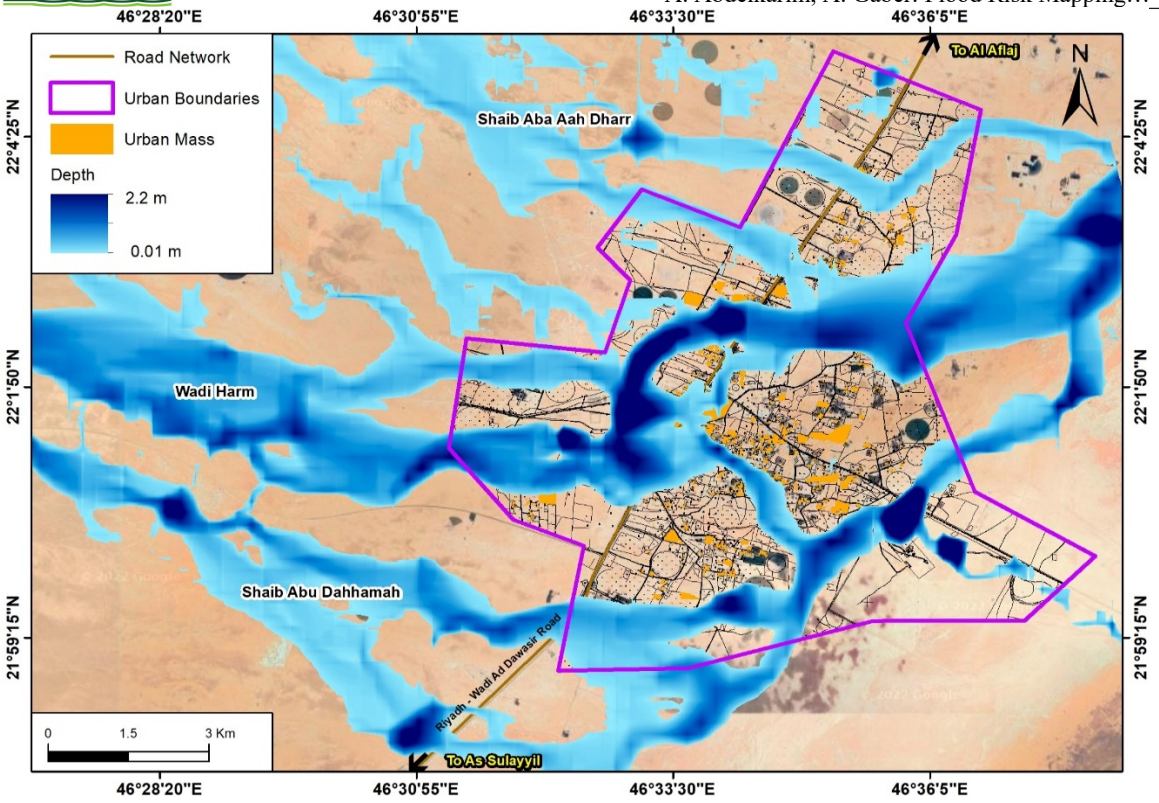

Fig. 17: Map of the depth of the flood waters of the valleys affecting the city of Al Bidi 100-year recurring period with the impact of climate change

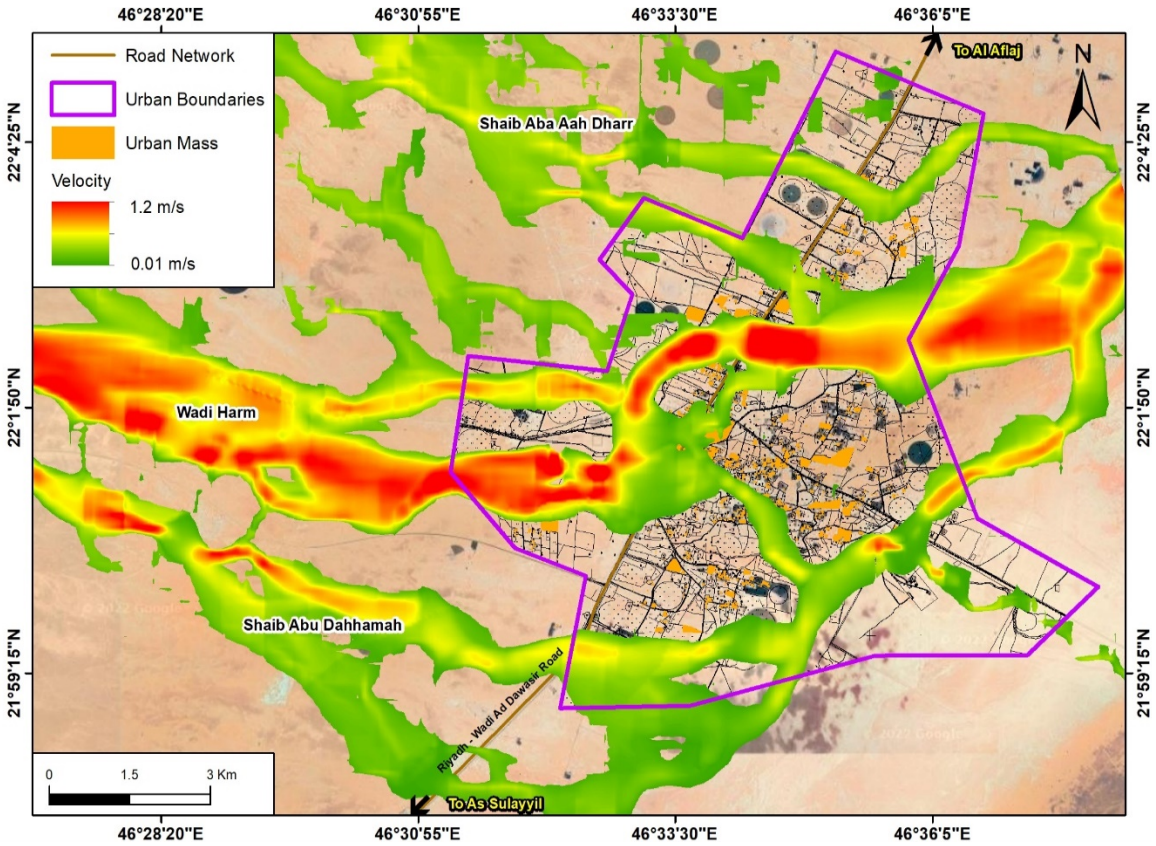

Fig. 18: Map of the velocity of the flood waters of the valleys affecting the city of Al Bidi 100-year recurring period with the impact of climate change

Source: the researcher's field work

Fig. 19: part of the field visit to validate the flood risk model

As indicated in the figures No. (20,21), the flow values, velocity sector, and depth of flow behind the bridge simulate what happened from an actual rainstorm, where the accuracy of the model reached around 92.5%, and it is clear from this that the model is highly efficient in simulating the actual situation of the rainstorm and its impact, which increases the degree of confidence in using the model prepared to study all areas exposed to the risks of torrential rain and rain and the proposed solutions of protection, drainage and network installations.

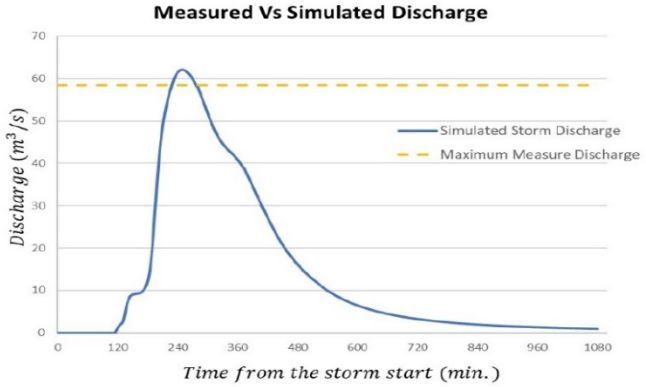

Fig. 20: The relationship between the measured and inferred flow quantity from hydraulic modeling at the existing bridge on Al Bidi -Wadi Ad Dawasir Road.

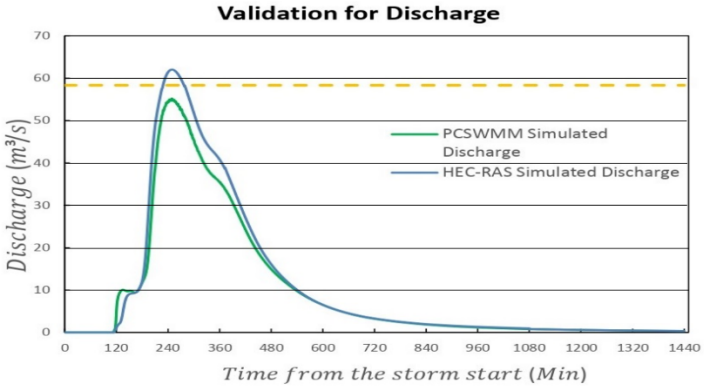

Fig. 21: Comparison of the flows resulting from (HEC-RAS) and (PC-SWMM) modeling at the existing bridge on Al Bidi - Wadi Ad Dawasir Road

The Frequency Ratio (FR) and Shannon's Entropy (SE) models have been combined to validation of the model of floods. These are the models most used in studies in the field of spatially and statistically validation of floods, This has confirmed many studies. the most important of which are studies: [46,47,48,49,50].

Figure (22) shows the flood validation curves for the FR and SE models, which correspond to a success accuracy of 88.55% and 85.22%. It was noted that both models in this study have demonstrated very good accuracy (08 to 0.7). It is an acceptable accuracy in most flood risk modeling studies.

3.7. Current Flood Risk Map:

Risk can be expressed as a combination of the probability of occurrence of damage and its consequences. Often, the risk is expressed by multiplying the value of the probability of a negative phenomenon and the value of the severity of its consequences. A similar equation is used to express the risk of flooding, but it is supplemented by other related values [51]. In this part, a visualization of the flood risks deduced from the two-dimensional hydraulic studies and the base map derived from the areal lift will be developed, and accordingly the three maps were calculated as follows:

3.7.1. Flood intensity map:

Flood risk maps provide clues to the area prone to flooding. Flood risk maps can be an effective tool to reduce damage through appropriate flood protection plans, and can be used for proper flood planning and forecasting [52], as clarified in figure no. (23).

3.7.2. Environmental sensitivity map:

Forecasting flood sensitivity can reduce mortality and economic losses from flood loss. Zoning of flood sensitive areas is a strategic component of any flood mitigation strategy [53,54]. The degree of sensitivity was calculated based on land uses for the base map. Al Bidi showed that it consists of agricultural and residential places, whereas agricultural places are not sensitive to floods like residential places, and Figure (24) indicates the degree of sensitivity for each site.

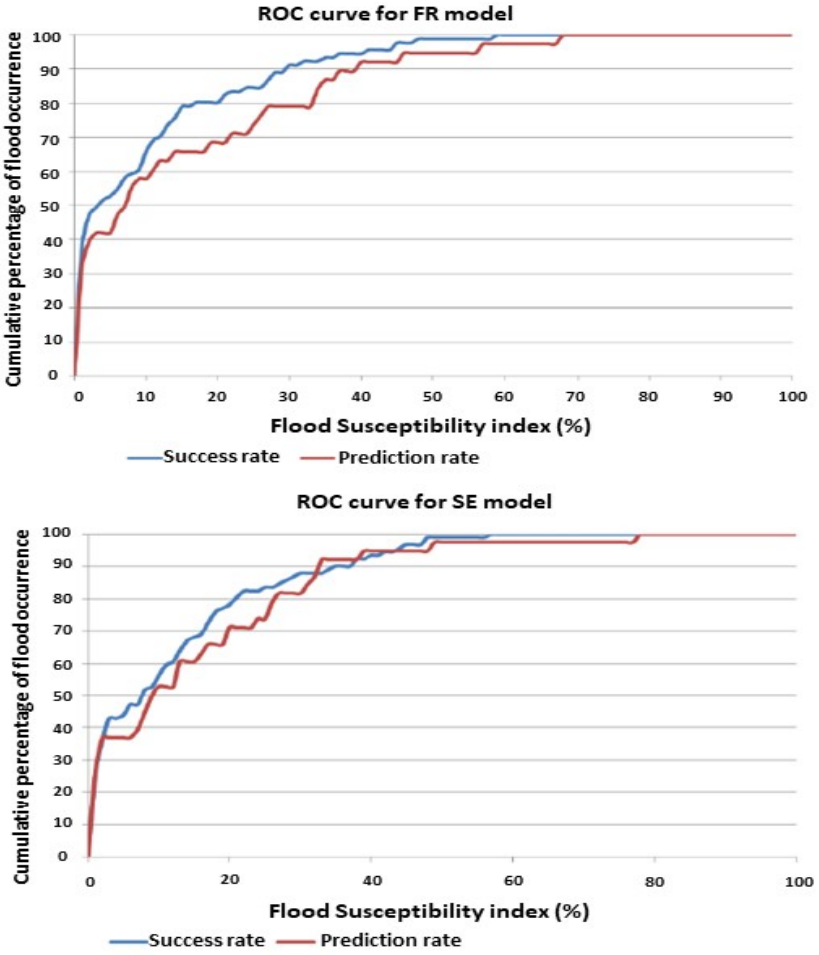

Fig. 22: ROC curve for (a) FR model and (b) SE model

3.7.3. Flood Risks map:

The flood risk map was calculated based on the hazard of the flood intensity and the sensitivity of the areas. The flood risk maps are a useful tool that helps in managing flood risks and identifying the flood area. The hydraulic model (HEC-RAS) is the best model for drawing flood inundation maps [55,56]. As indicated in Figure No. (25), the city center is the most vulnerable place, due to the overcrowding of the population, which increased the degree of sensitivity, as well as the speed and depth of flooding in this area. Accordingly, it can be concluded that the National Center and schemes 525 and 433 are among the places most exposed to a clear risk.

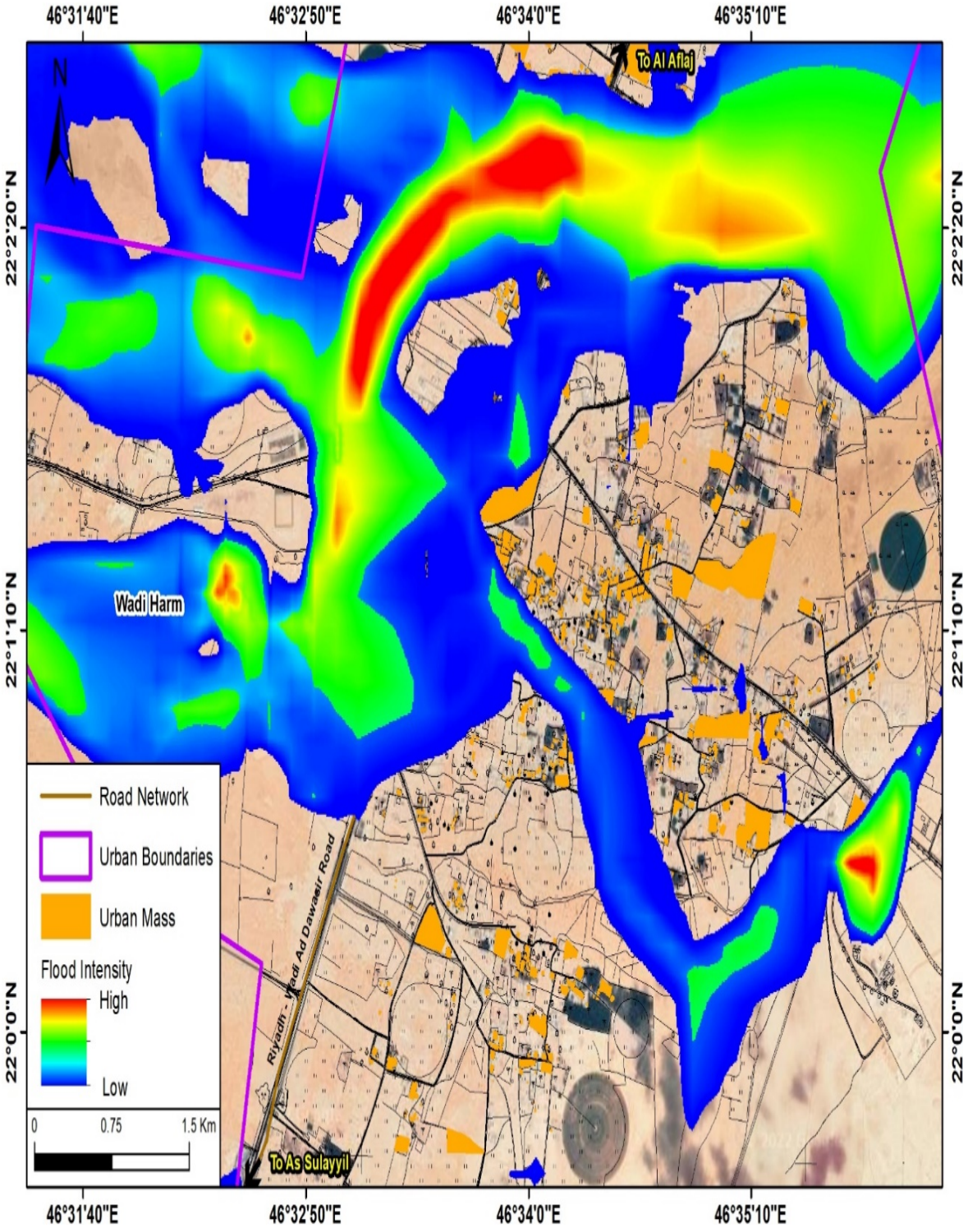

Fig. 23: Flood intensity map of Al Bidi City

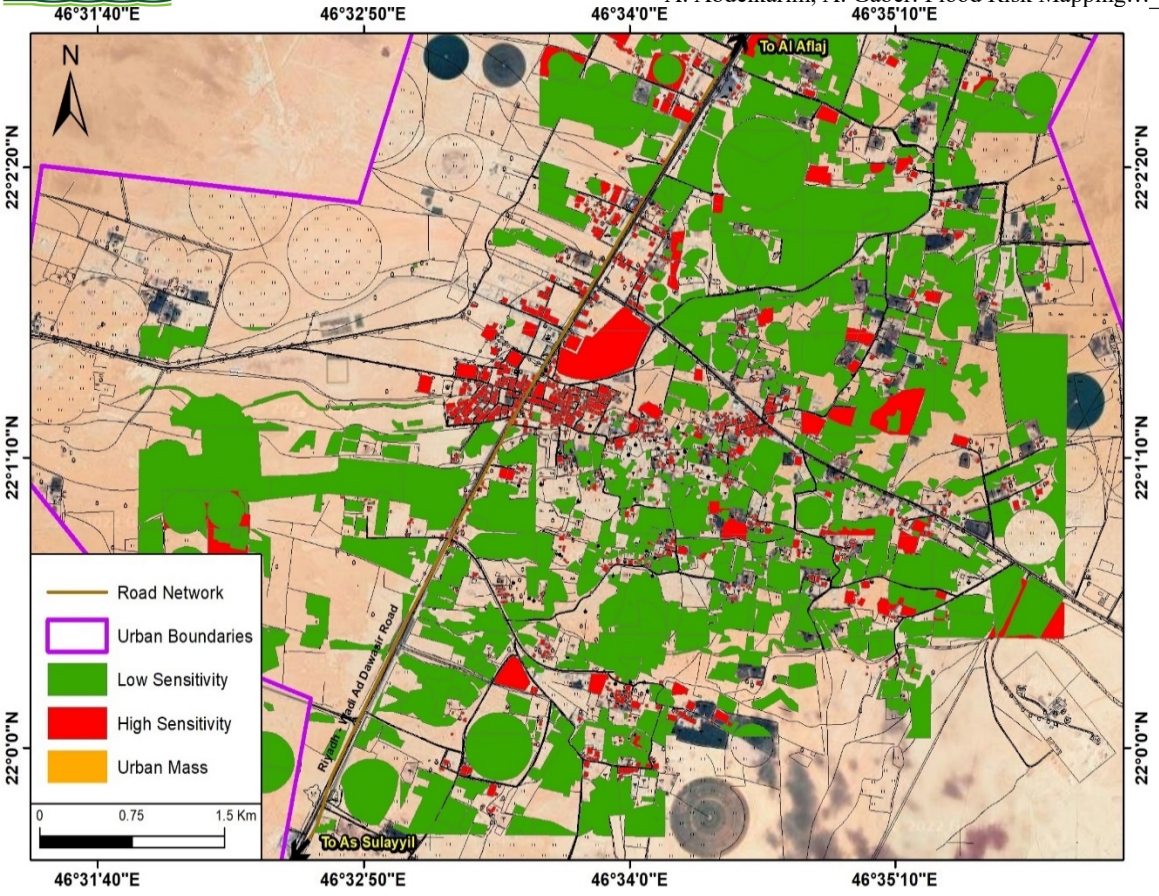

Fig. 24: Degree of environmental sensitivity map in Al Bidi City

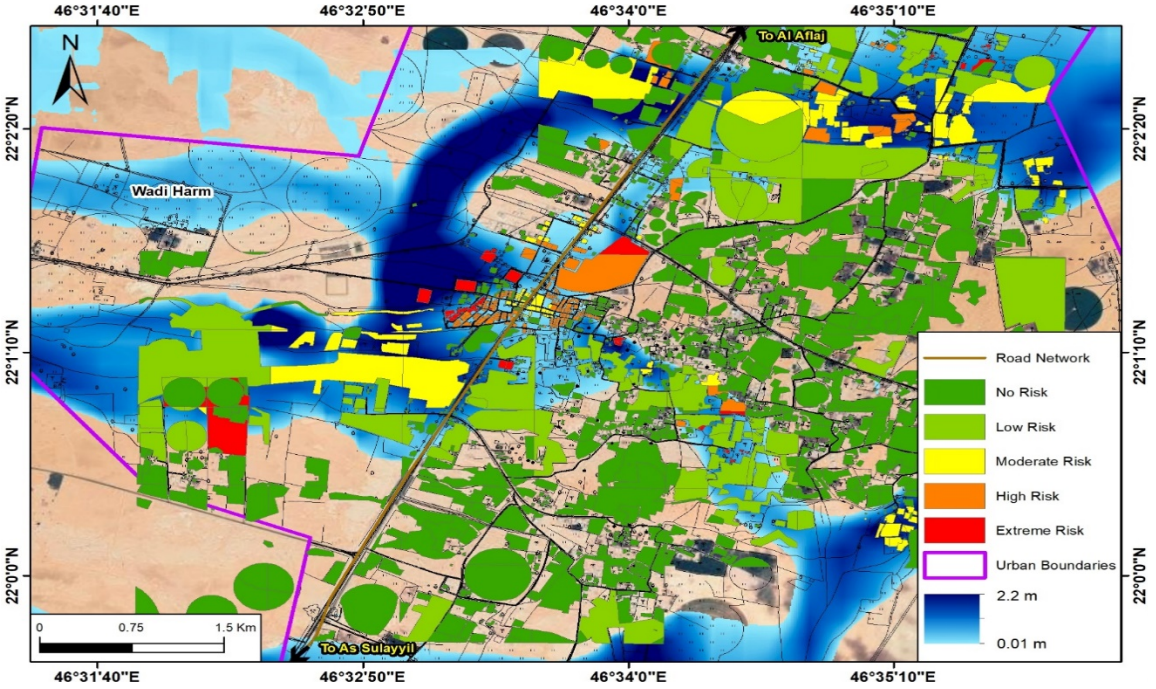

Fig. 25: Flood risk map of Al Bidi City

3.8. Assessment of facilities to eliminate risks in Al Bidi City:

It became clear from the survey work of Al Bidi city that there are three types of facilities to eliminate the risks of floods: culverts, Embankments, and an Tranquilization Lake. They will be discussed in detail as follows:

3.8.1. Existing culverts:

All existing culverts in figure No. (26) were evaluated, and it was found that the culverts (EX08-(M-14) & EX09-(M15)) are unsafe and incapable of passing valley flows, but do not need alternative culverts since the proposed solutions fulfill the required purpose, while the culvert (EX19-(M25)) is an unsafe culvert, but needs to increase one opening with the same dimensions, and as it turned out that most of the existing culverts drain small reefs water and do not fall on major valleys.

Source: the researcher's field work

Fig. 26: sample of the existing culverts in the city of Al Bidi, where (a) a model for tube culverts, (b) a model for box culverts

3.8.2. Existing Embankments:

It became clear from the actual survey works that there are three existing Embankments, Figures No. (27,28), while Table No. (9) indicates the characteristics of the Embankments. The results of the hydraulic modeling showed that the Embankment No. 1 and 2 are useless because the limits of the flood are greater than to be contained by such Embankments, and therefore these Embankments are not safe, and that Embankment No. 3 is not safe because of the 2.8 meters high water resulting from the flooding of Wadi Harm, while the height of Embankments is only 1.5 meters. Figure No. (29).

Table 9: Characteristics of the existing Embankments

Embankments no.	**Embankments length (m)**	**Embankments height (m)**	**Embankments width (m)**
Embankments no. 1	397.627	2	9
Embankments no. 2	252.197	2	9
Embankments no. 3	1183.984	1.50	9

Source: the researcher's field work

Fig. 27: Models of the existing Embankments from the actual survey works, where (a) Embankment No. 1, (b) Embankment No. 2, (c) Embankment No. 3

3.8.3. Tranquilization Lake and Embankment of the Tranquilization Lake:

It became clear from the actual survey that there is an Tranquilization Lake and Embankment to the west of Al Bidi city, which is around 20 km. Figures No. (30,31) and tables No. (10,11) indicate the characteristics of the Tranquilization Lake and Embankment. The Tranquilization Lake was modeled on the program (HEC-HMS), and it was found that the Tranquilization Lake does not contain the entire volume of the incoming flow of 170 m^3/s, and it discharges 110 m^3/s. Figure no. (32) shows the lake's hydrograph and flow.

Table 10: Characteristics of the Tranquilization Lake

Tranquilization Lake	lake length (m)	lake width (m)	lake area (m^2)
Tranquilization Lake	720	860	619200

Table 11: Characteristics of the existing Embankment of the Tranquilization Lake

Embankment no.	Embankment length (m)	Embankment height (m)	Embankment width (m)
existing Embankment of the Tranquilization Lake	1200	1.9	13.4

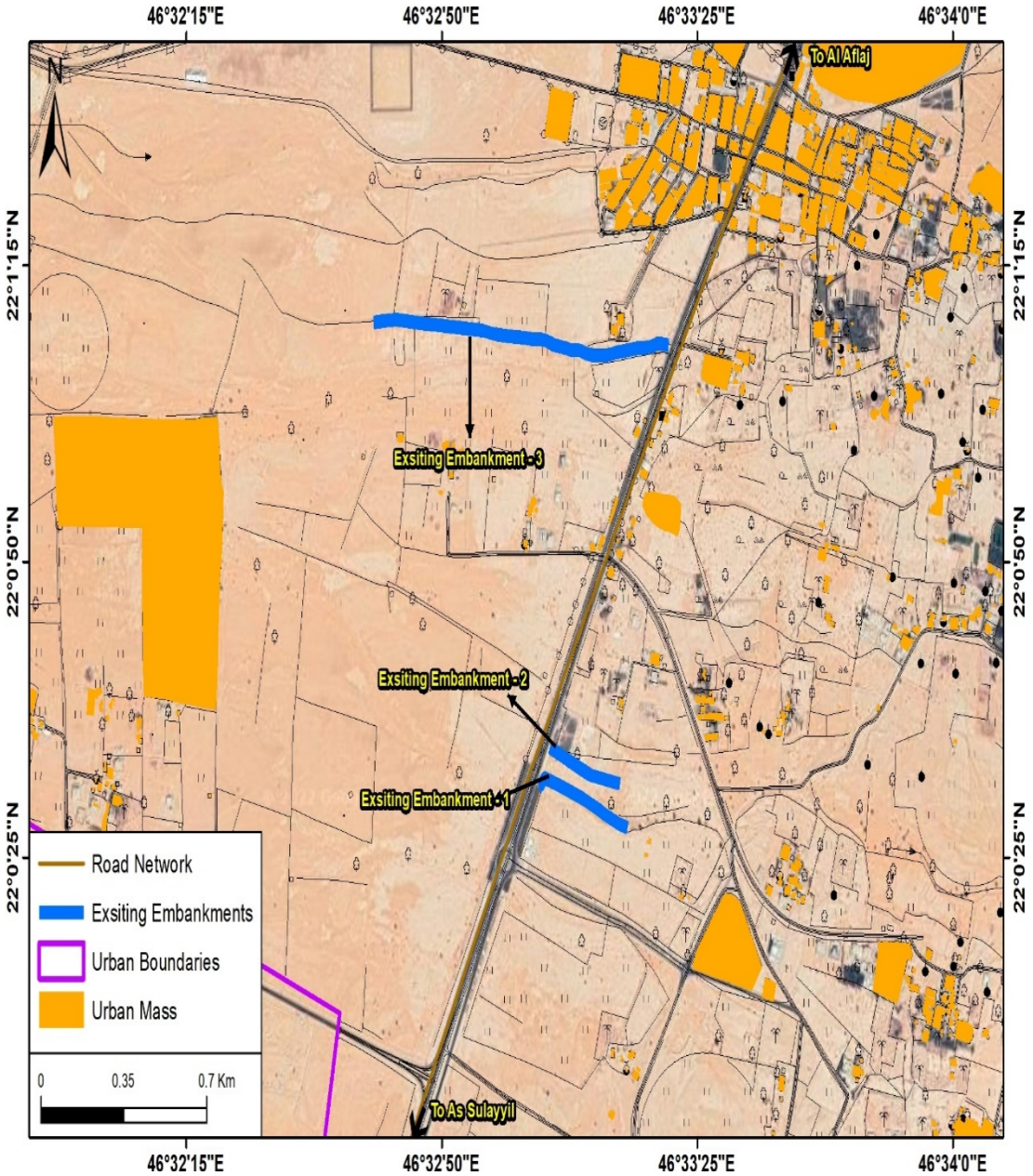

Fig. 28: Installations to prevent the risks of existing floods (Embankment) from the actual survey works

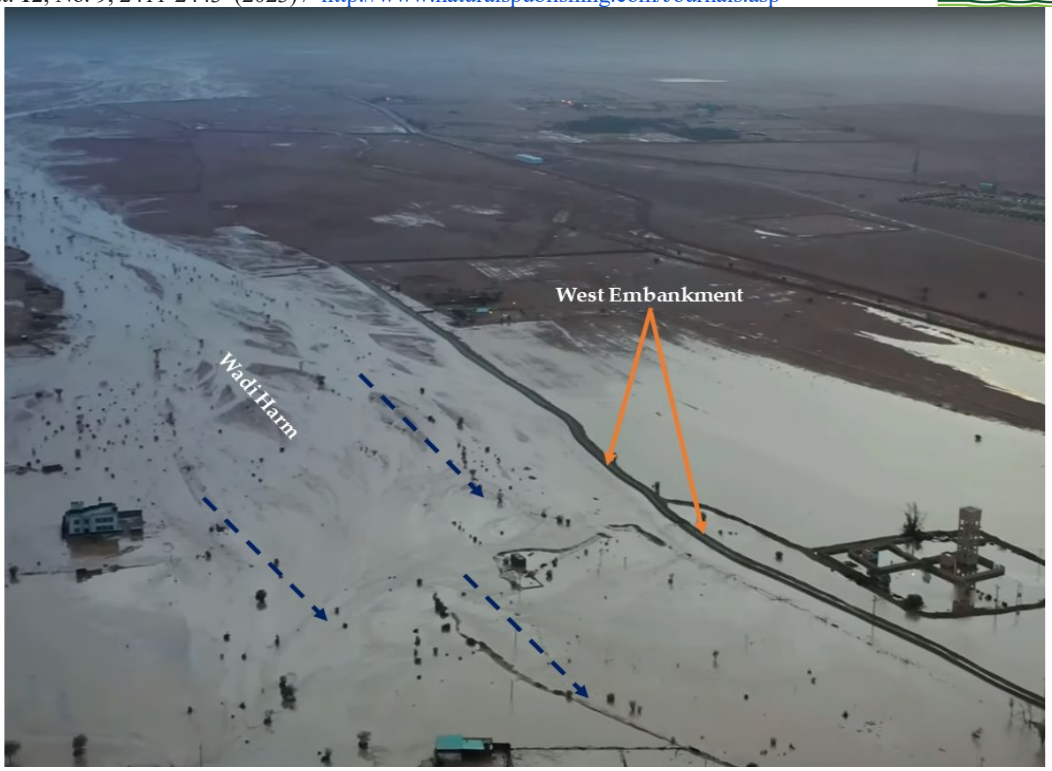

Source: https://sabq.org/saudia/nhgrh9

Fig. 29: the impact of Wadi Harm floods on the city of Al Bidi, which indicates the Embankment that directed the water into the city with a negative effect on 18/07/2021

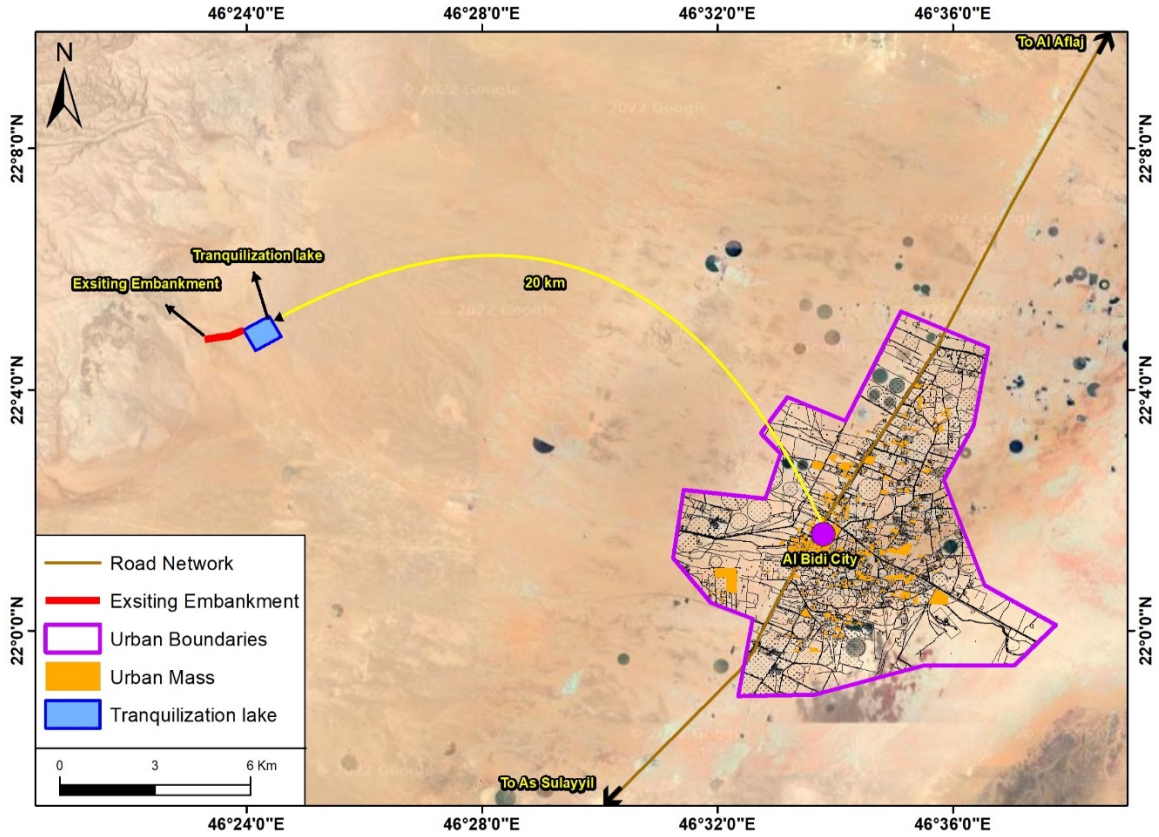

Fig. 30: The location of the Tranquilization Lake in Al Bidi from the actual survey works

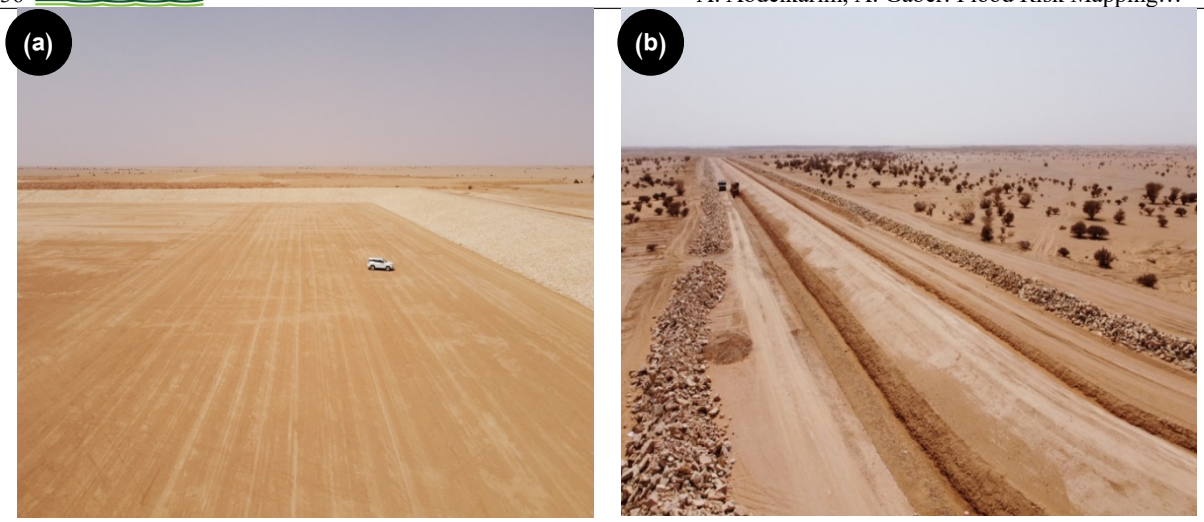

Source: the researcher's field work

Fig. 31: Tranquilization Lake and the Embankments of the Alleviation Lake from the actual survey mylar, whereas (a) the Tranquilization Lake, (b) the Embankments of the Tranquilization Lake

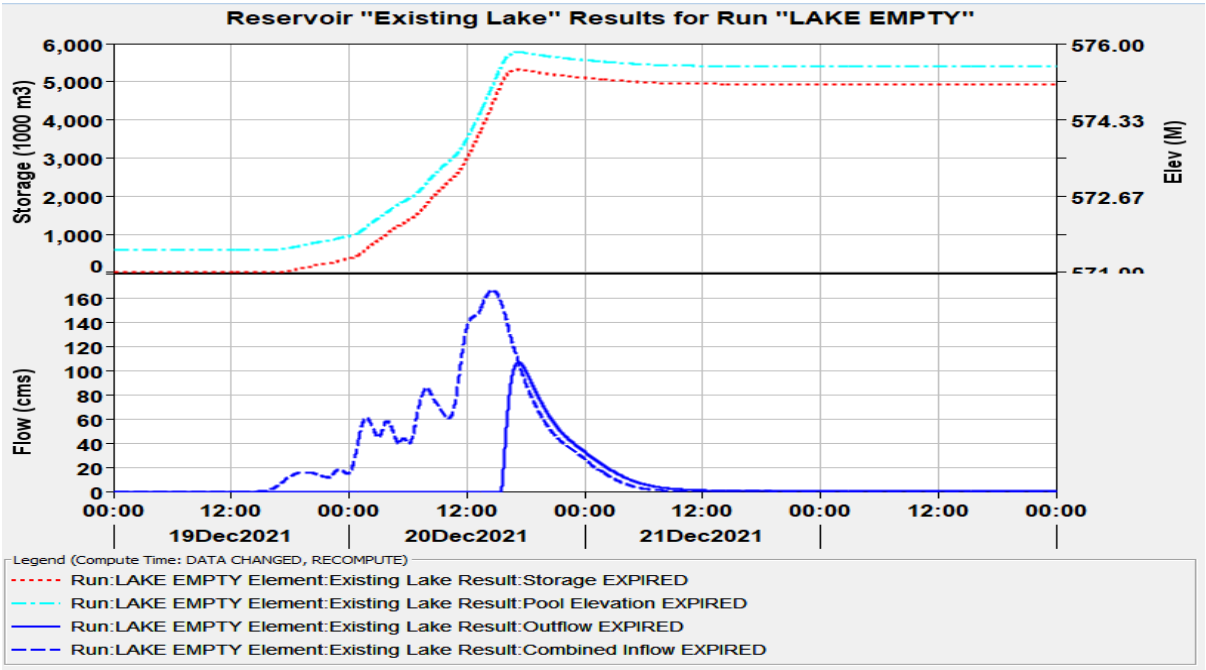

Fig. 32: indicates the incoming and outgoing flow from the lake

3.9. Suggested design scenarios for the mitigation strategy:

After studying the city of Al Bidi, it was found out that the main threat to the town is the flow coming from Wadi Harm, and because of the nature of the plain area and the absence of topography or natural obstacles; the flows coming from the valley cause the city to sink and threaten lives and property. Satellite images have shown the presence of a much industrial Embankment that the town's residents built. Still, the photos taken of the city during the floods show the futility of this Embankment, and despite their large number, they cannot control the flood water.

The existing lake, far west of Al Bidi city, was evaluated, and it was found that it does not absorb the entire flow of the valley for a 100-year design storm. Accordingly, two design scenarios were concluded, and in this part, the two scenarios will be presented: the selected scenario and the reason for selection.

3.9.1. First Scenario:

In this scenario, it is assumed that the lake is empty, and then the lake can contain part of the flow until it is filled, and

the rest of the flow is passed when the maximum volume of lake filling is reached, and this scenario is considered the best. Figures (33,34) show the impact of the empty lake on the final hydrograph at City.

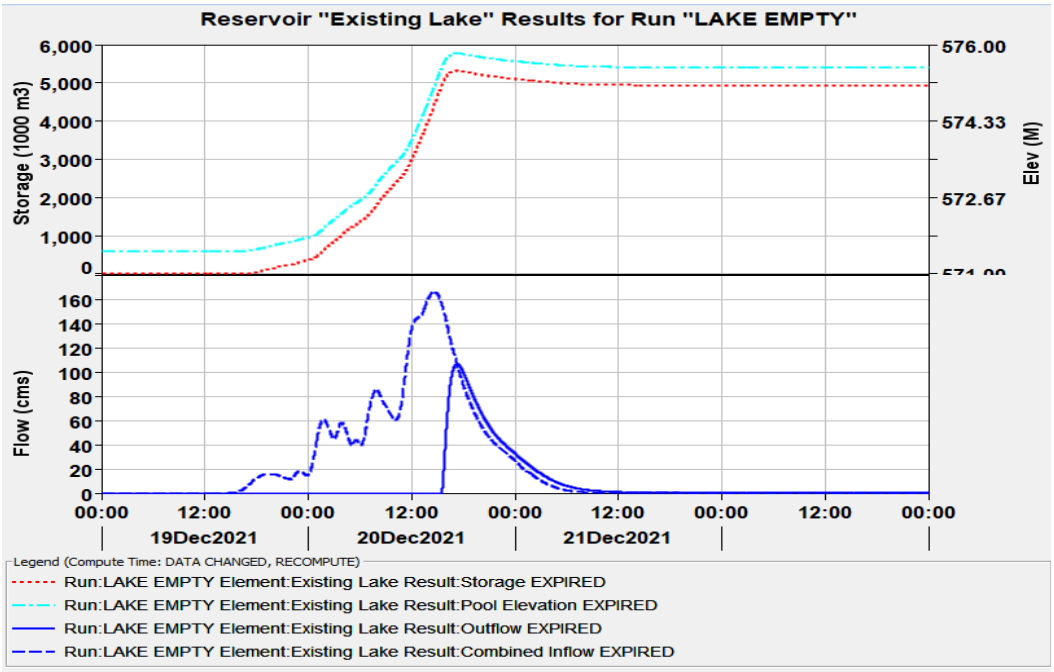

Fig. 33: indicates the outflow from the previously empty lake

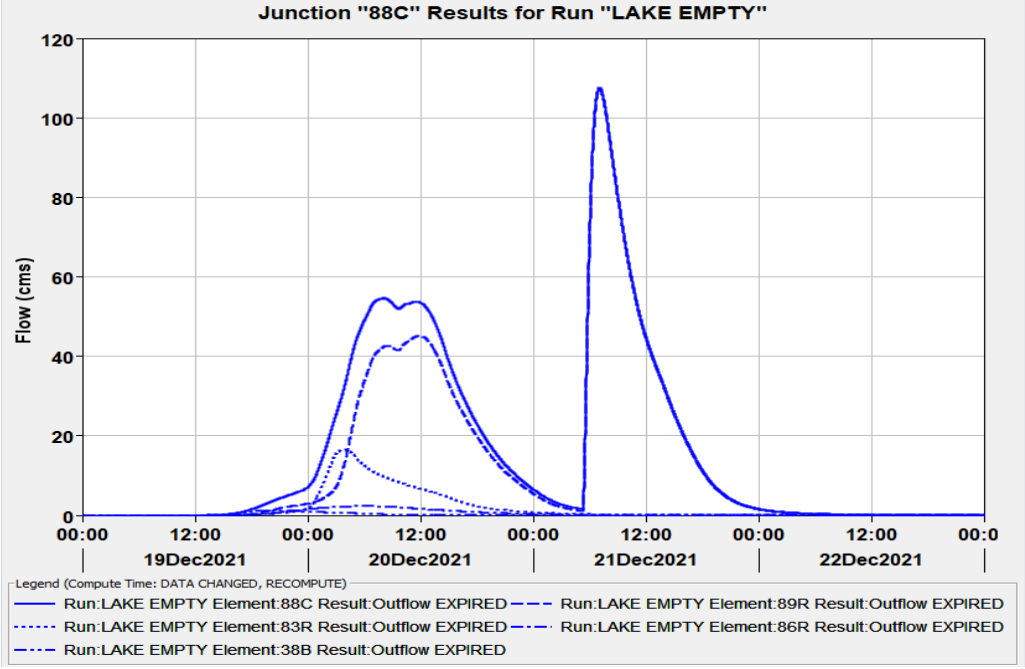

Fig. 34: shows the final flow at the city (point 88C) inferred from the previously empty lake

3.9.2. The second scenario:

In this scenario, it was assumed that the lake is filled, and this is likely to happen if more than one storm occurs in a short time, so the lake cannot absorb any flow before the 100-year storm occurs, and this leads to the passage of the entire flow without sequestering any water from it. This scenario is considered the worst, and Figures (35,36) indicate the impact of a pre-filled lake on the final hydrograph in the city.

As a result of the analysis, the flows were deduced according to Table No. (12). Accordingly, the design was based on the inferred flows from the second scenario, as it is a critical scenario that may lead to catastrophic results when it

occurs, and this is what happened in the recent torrential rains that hit the city on 18/7/2021, as the lake could not contain the entire flow, which led to the city's being completely submerged.

Table 12: Modeling Scenarios and Calculated Flow of the Existing Lake

Scenarios	Lake condition	Maximum outflow from the lake (m^3/s)	Scenario condition	Remarks
Scenario 1	empty	110	Best scenario	In this scenario we assume that the lake is empty and therefore can contain part of the flow
Scenario 2	Filled	170	Worst scenario	In this scenario we assume that the lake is full and then the entire flow will pass without affecting the lake

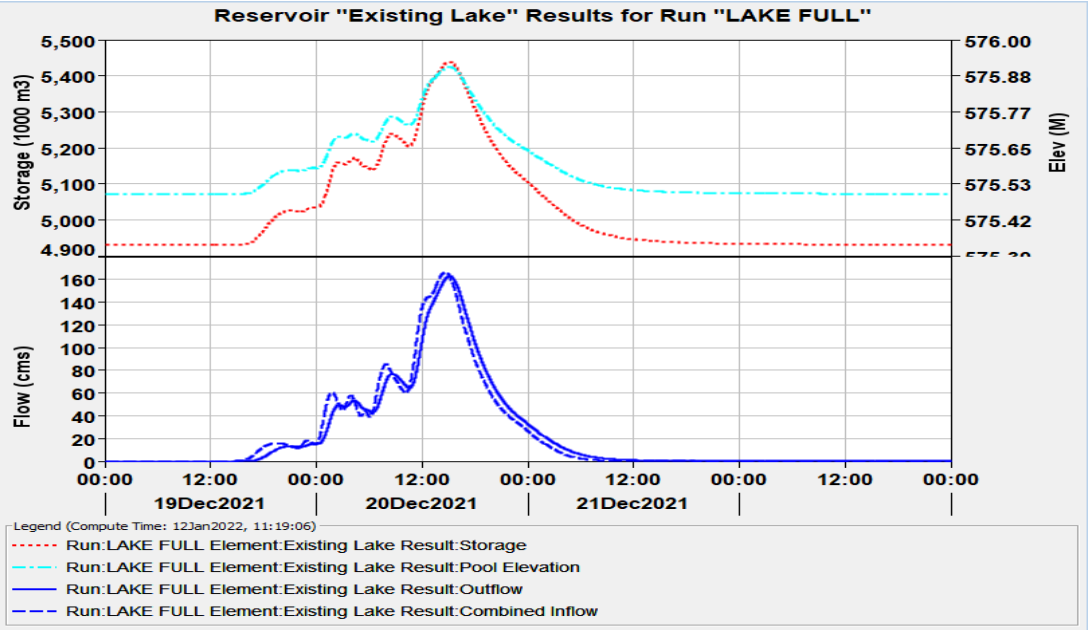

Fig. 35: Indicates the outflow from a previously filled lake

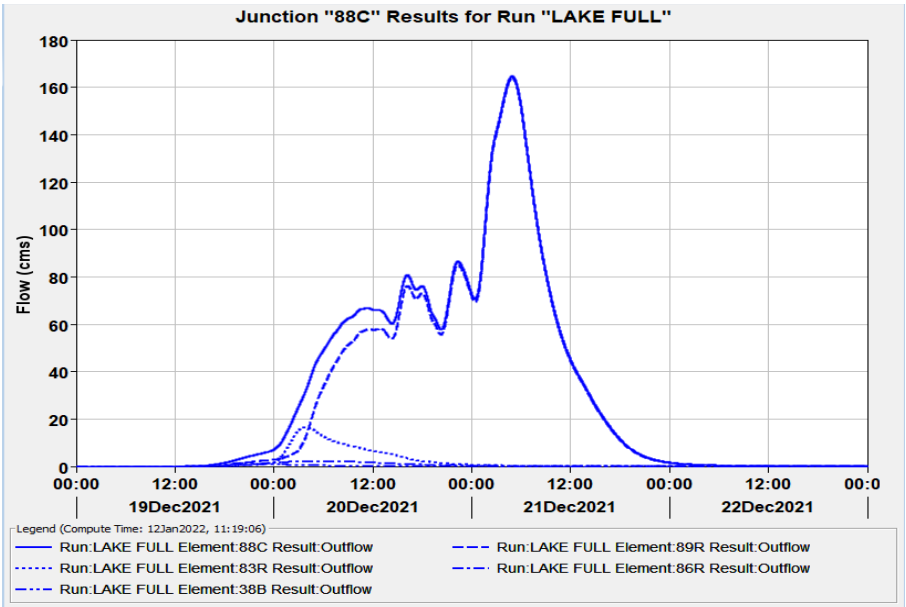

Fig. 36: The final flow at the city (point 88C) inferred from the previously filled lake

3.10. The proposed protection and prevention plan against flood risks for the city:

The protection and prevention plan proposed by the researcher to eliminate the risks of floods in the city of Al Bidi is based on a proposal to make two Embankments pass water between them safely; the first Embankment with a length of 5940 meters and the second Embankment with an altitude of 7210 meters and a height of 2.5 meters for both, to transfer the water of the southern valleys (Wadi Harm) to the industrial channel through the two proposed culverts at the intersection of the industrial channel with the existing road. The characteristics of these culverts represent having eight slots, 3 meters wide and 3 meters high, to safely drain the valleys' water, in addition to the proposal of two industrial channels, the first with a length of 6075 meters, the width of 10 meters, and an average depth of 4 meters. The second channel is 13,950 meters long, 4 meters wide, with an average depth of 2 meters, to pass the waters of the northern valleys into the proposed Embankments. Figure No. (37) indicates the plan for protection and prevention of flood risks for Al Bidi.

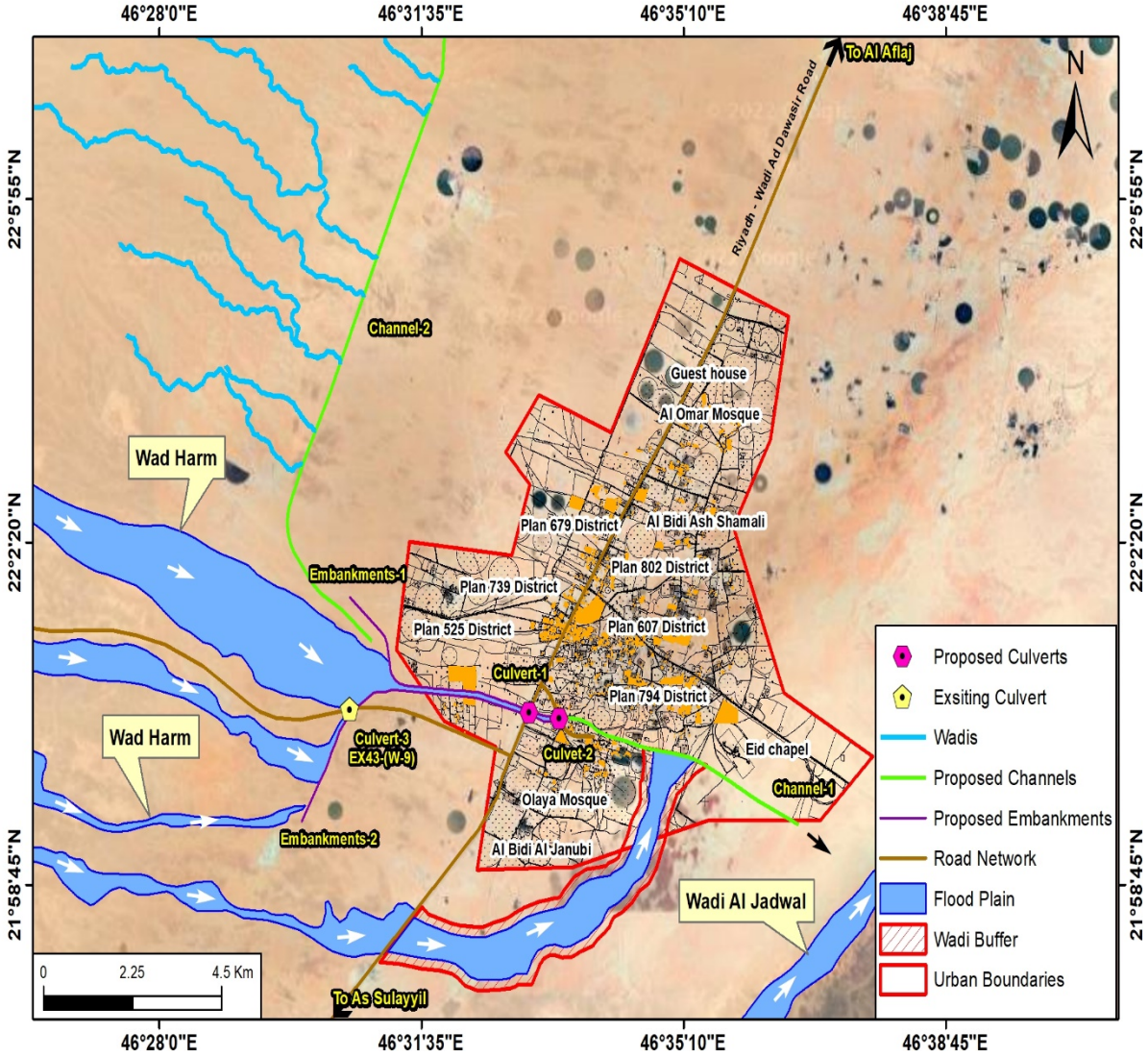

Fig. 37: The proposed protection and prevention plan against flood risks for Al Bidi City

4 Discussion and Conclusions:

The flood risk map was produced based on an integrated approach for integrating geomatics represented in remote sensing (RS), geographic information systems (GIS), and modeling Hydrodynamics through the development of three integrated maps: flood intensity, environmental sensitivity, and flood risks maps revealed that the city of Al Bidi is exposed to torrential risks transmitted from the west to the east due to the presence of a group of significant valleys such as Wadi Harm, of which the sources start from the west towards the east directly towards the city, and these valleys result in sudden floods and torrents, whereas around 60% of the urban area of Al Bidi city is flooded with torrential

water, where the flows of valleys affecting the study area range between 1.50 m^3/s and 170 m^3/s, depths ranging between 0.01-2.2 meters, and velocity ranging between 0.01-1.2 meters per second**.** It was also found that the city center is the most vulnerable place due to the overcrowding of the population, which increased the degree of sensitivity, as well as the velocity and depth of the flood in this area. Accordingly, it can be concluded that the National Center and schemes 525 and 433 are among the places most exposed to clear danger and that the presence of four central valley's coming from west to east carrying millions of cubic rain from torrential water runoff is lost every year without benefiting from them, in addition to the destruction of infrastructure in light of the inability of the existing culverts in the city of Al Bidi to contain the passing flow and the blockage of some of them due to the remnants of the torrents during their flow and their inability to drain the incoming floods abundantly. Wadi Harm, Wadi Al Hinu, Wadi Al Jadwal, and Shaib Ab Ash Darr, are what projects should be directed to eliminate the risks of torrents instead of waiting for the streams to reach the Al Bidi city.

The flood disasters that occurred in urban areas in Al Bidi city as a model for the Saudi city, which is located in the arid and semi-arid environment, were associated with several urban and environmental challenges, which helped to increase the severity and risk of the flood risks in the study area. Perhaps the most important of these challenges is the lack of data, the restrictions imposed on them, the unique characteristics of valleys, the excessive urban expansion, the establishment of ill-considered urban plans, the lack of projects implemented to eliminate the risks of torrential rains, the lack of balance between the construction of dams and the provision of water, which is the primary source of groundwater and agriculture, and the failure to use suitable and heterogeneous hydrodynamic models in the preparation of hydrological and hydraulic studies; especially the two-dimensional models that depend on parameters such as velocity, depth, and spatial spread, which were applied in this study such as (PCSWMM (2D)) and (HEC-RAS) models. These models are suitable for the examination of flood risks in urban areas. The lack of accurate maps of the risk dangers of floods for most Arab cities and a lack of strategic planning for risks exacerbated the crisis. Undoubtedly, the global climate change and severe weather affected the nature and form of seasonal and local rains in the study area, which helped to increase the surface runoff of valleys in arid and semi-arid environments. The current trend and future scenarios for flood risks in the Arab city require obtaining accurate spatial and temporal information about the potential dangers of floods, through the production and mapping of potential flood risks, especially in Arab towns located in the estuaries of the valleys, the proximity of ravines, and the adoption of new urban plans only in the light of detailed studies of flood risk maps.

Undoubtedly, the integration of geomatics represented by remote sensing and GIS combined with hydrodynamic modeling helped provide a platform for collecting, analyzing, treating, evaluating, and managing flood-prone areas very quickly and efficiently in this study.

The study recommends the necessity of engineering intervention through the transfer of the torrents of Wadi Harm by constructing two Embankments, a channel and a group of culverts, and the disposal of flood waters in Wadi Al Jadwal located to the east of the city and proposing two industrial channels to pass the northern valleys into the proposed Embankments.

The study also recommends directing the future urban growth and infrastructure of the study area away from the areas referred to in the flood risk map, which the study concluded as high and very high-risk regions with the prohibition of construction in these areas and not expanding in agricultural areas except after providing mechanisms to eliminate the risks of floods commensurate with the nature of the flow of valleys out.

Although the current study deals with the drainage basins of Al Bidi city; a similar approach can be implemented in identical drainage basins in urban areas in arid and semi-arid environments, and the results may be helpful for planners to define priorities for protection from flood risks and to prepare an early warning system for floods.

Funding:

This research has not received any financial support.

Conflicts of Interest:

The authors declare no conflicts of interest.

References:

[1] A. Abdelkarim, S. Al-Alola, H. Alogayell, S. Mohamed, I. Alkadi, and I. Youssef, "Mapping of GIS-Flood Hazard Using the Geomorphometric-Hazard Model: Case Study of the Al-Shamal Train Pathway in the City of Qurayyat, Kingdom of Saudi Arabia," *MDPI, Geosciences*, Vol. 10, No. 9, pp .1-32, 2020.

[2] M. Abdel-Fattah, M. Saber, S. A. Kantoush, M. F. Khalil, T. Sumi, and A. A. Sefelnasr, "Hydrological and Geomorphometric Approach to Understanding the Generation of Wadi Flash Floods," *MDPI, Water*, Vol. 9, No. 7, pp. 11-27, 2017.

[3] G. Bathrellos, E. Karymbalis, H. Skilodimou, K. Gaki-Papanastassiou, and E. Baltas, "Urban flood hazard assessment in the basin of Athens Metropolitan City, Greece," *Environmental Earth Sciences*, Vol. 75, no. 4, pp. 1-14, 2016.

[4] A. Ramachandran, K. Palanivelu, B. Mudgal, A. Jeganathan, S. Guganesh, B. Abinaya, and A. Elangovan, "Climate change impact on fluvial flooding in the Indian sub-basin: A case study on the Adyar sub-basin," *PLOS ONE Journal*, Vol. 14, no. 5, pp. 1-24, 2019.

[5] D. Tadesse, K. Suryabhagavan, D. Nedaw, and B. Hailu, "A model-based flood hazard mapping in Itang District of the Gambella region, Ethiopia," *Geology, Ecology, and Landscapes*, pp. 1-18, 2022.

[6] H. Hong, P. Tsangaratos, I. Ilia, J. Liu, A. Zhu, and W. Chen, "Application of fuzzy weight of evidence and data mining techniques in construction of flood susceptibility map of Poyang County, China," *Science of The Total Environment*, Vol. 625, pp. 575–588, 2018.

[7] F. Perosa, L. Seitz, A. Zingraff-Hamed, and M. Disse, "Flood risk management along German rivers – A review of multi-criteria analysis methods and decision-support systems," *Environmental Science & Policy*, Vol. 135, pp. 191-206, 2022.

[8] M. Al-Zahrani, A. Al-Areeq, and H. Sharif, "Estimating Urban Flooding Potential Near the Outlet of An Arid Catchment in Saudi Arabia," *Geomatics, Natural Hazards and Risk*, Vol. 8, Issue 2, pp. 672–688, 2017.

[9] A. Abdelkarim, and A. Gaber, "Flood Risk Assessment of the Wadi Nu'man Basin, Mecca, Saudi Arabia (During the Period, 1988–2019) Based on the Integration of Geomatics and Hydraulic Modeling: A Case Study," *MDPI, Water*, Vol. 11, no. 9, pp. 1-32, 2019.

[10] A. Abdelkarim, D. Gaber, I. Alkadi, and H. Alogayell, "Integrating Remote Sensing and Hydrologic Modeling to Assess the Impact of Land-Use Changes on the Increase of Flood Risk: A Case Study of the Riyadh–Dammam Train Track, Saudi Arabia," *Sustainability, MDPI*, Vol. 11, no. 21, pp. 1-32, 2019.

[11] J. Lee, E. Kang, and S. Jeon, "Application of frequency ratio model and validation for predictive flooded area susceptibility mapping using GIS," *IEEE International Geoscience and Remote Sensing Symposium*, pp. 895–898, 2012.

[12] S. Tehrany, B. Pradhan, and N. Jebur, "Flood susceptibility analysis and its verification using a novel ensemble support vector machine and frequency ratio method," *Stochastic Environmental Research and Risk Assessment*, Vol. 29, pp. 1149–1165, 2015.

[13] S. Stefanidis, and D. Stathis, "Assessment of flood hazard based on natural and anthropogenic factors using analytic hierarchy process (AHP)," *Natural Hazards*, Vol. 68, pp. 569–585, 2013.

[14] B. Pradhan, "Use of GIS-based fuzzy logic relations and its cross application to produce landslide susceptibility maps in three test areas in Malaysia," *Environmental Earth Sciences*, Vol. 63, pp. 329–349, 2011.

[15] B. Pradhan, "Flood susceptible mapping and risk area delineation using logistic regression, GIS and remote sensing," *Journal of Spatial Hydrology,* Vol. 9, no. 2, pp. 1–18, 2010.

[16] M. Saeed, H. Li, S. Ullah, A. Rahman, A. Ali, R. Khan, W. Hassan, I. Munir, and S. Alam, "Flood Hazard Zonation Using an Artificial Neural Network Model: A Case Study of Kabul River Basin, Pakistan," *Sustainability, MDPI*, Vol. 13, pp. 1-21, 2021.

[17] S. Elsafi, "Artificial Neural Networks (ANNs) for flood forecasting at Dongola Station in the River Nile ,Sudan," *Alexandria Engineering Journal*, Vol. 53, Issue 3, pp. 655–662, 2014.

[18] S. Siahkamari, A. Haghizadeh, H. Zeinivand, N. Tahmasebipour, and O. Rahmati, "Spatial prediction of flood-susceptible areas using frequency ratio and maximum entropy models," *Geocarto International*, Vol. 33, Issue 9, pp. 927–941, 2018.

[19] S. Samanta, D. Pal, and B. Palsamanta, "Flood susceptibility analysis through remote sensing, GIS and frequency ratio model". *Applied Water Science*, Vol. 8, pp. 1–14, 2018.

[20] A. Abdelkarim, A. Gaber, A. Youssef, and B. Pradhan, "Flood Hazard Assessment of the Urban Area of Tabuk City, Kingdom of Saudi Arabia by Integrating Spatial-Based Hydrologic and Hydrodynamic Modeling", *MDPI,*

Sensors, Vol. 19, no. 5, pp. 1-23, 2019.

[21] A. Abdelkarim, M. M. Awawdeh, H. M. Alogayell, and S. Al-Alola, "Integration of Remote Sensing, Hydrological and Hydraulic Modeling for Flood Risk Assessment and Mitigation in The Coastal City of Al-Lith, Saudi Arabia," *International Journal of GEOMATE*, Vol. 18, no. 70, pp. 252-280, 2020.

[22] A. Abdelkarim, "Assessment of the expected flood hazards of the Jizan-Abha Highway, Kingdom of Saudi Arabia by Integrating Spatial-Based Hydrologic and Hydrodynamic Modeling," *The Global Journal of Researches in Engineering*, Vol. 19, Issue 4, pp. 27-55, 2019.

[23] L. Sidek, L. Chua, A. Azizi, H, Basri, A. Jaafar, and W. Moon, "Application of PCSWMM for the 1-D and 1-D–2-D Modeling of Urban Flooding in Damansara Catchment, Malaysia," *Applied Sciences, MDPI*, Vol. 11, pp. 1-16, 2021.

[24] J. Shireman, K. Ratliff, and A. Mikelonis, "Modeling radionuclide transport in urban overland flow: a case study," *Urban water Journal*, Vol. 19, no. 2, pp. 130-140, 2021.

[25] F. Liwanag, D. Mostrales, M. Ignacio, and J. Orejudos, "Flood Modeling Using GIS and PCSWMM", *Engineering Journal*, Vol. 22, no. 3, pp. 279-289, 2018.

[26] A. Hjelmstad, A. Shrestha, M. Garcia, and G. Mascaro, "Propagation of radar rainfall uncertainties into urban pluvial flood modeling during the North American monsoon," *Hydrological Sciences Journal*, Vol. 66, no. 15, pp. 2232-2248, 2021.

[27] X. Fang, D. B. Thompson, T. G. Cleveland, P. Pradhan, and R. Malla, "Time of Concentration Estimated Using Watershed Parameters Determined by Automated and Manual Methods," *Journal of Irrigation and Drainage Engineering*, Vol. 134, Issue 2, pp. 202-211, 2008.

[28] D. Sultan, A. Tsunekawa, M. Tsubo, N. Haregeweyn, E. Adgo, D. T. Meshesha, A. A. Fenta, K. Ebabu, M. L. Berihun, and T. A. Setargie, "Evaluation of lag time and time of concentration estimation methods in small tropical watersheds in Ethiopia," *Journal of Hydrology: Regional Studies*, Vol. 40, pp. 1-14. 2022.

[29] S. Roy, and B. Mistri, "Estimation of Peak Flood Discharge for an Ungauged River: A Case Study of the Kunur River, West Bengal," *Geography Journal*, Vol. 2013, pp. 1-12, 2013.

[30] H. Sharif, F. Al-Juaidi, A. Al-Othman, I. Al-Dousary, E. Fadda, S. Jamal-Uddeen, and A. Elhassan, "Flood hazards in an urbanizing watershed in Riyadh, Saudi Arabia," *Geomatics, Natural Hazards and Risk*, Vol. 7, no. 2, pp. 702-720, 2016.

[31] A. Feldman, "Hydrologic modeling system HECHMS: technical reference manual," *USACE (United States Army Corps of Engineers)*, pp. 1-148, 2000.

[32] C. Fan, H. Ko, and S. Wang, "An innovative modeling approach using Qual2K and HEC-RAS integration to assess the impact of tidal effect on River Water quality simulation," *Journal of Environmental Management*, Vol. 90, Issue 5, pp. 1824–1832, 2009.

[33] K. van Ginkel, F. Dottori, L. Alfieri, L. Feyen, and E. Koks, "Flood risk assessment of the European road network," *Natural Hazards and Earth System Sciences*, Vol. 21, pp. 1011–1027, 2021.

[34] M. Horritt, and P. Bates, "Evaluation of 1D and 2D Numerical Models for Predicting River Flood Inundation," *Journal of Hydrology*, Vol. 268, Issue 1-4, pp. 87–99, 2002.

[35] M. Anderson, Z. Chen, M. Kavvas, and A. Feldman, "Coupling HEC-HMS with atmospheric models for prediction of watershed runoff," *Journal of Hydrologic Engineering*, Vol. 7, Issue 4, pp. 312–318, 2002.

[36] Q. Siddiqui, N. Hashmi, and R. Ghumman, "Flood inundation modeling for a watershed in the pothowar region of Pakistan," *Arabian Journal for Science and Engineering*, Vol. 36, pp. 1203–1220, 2011.

[37] M. Ferri, U. Wehn, L. See, M. Monego, and S. Fritz, "The Value of Citizen Science for Flood Risk Reduction: Cost-benefit Analysis of a Citizen Observatory in the Brenta-Bacchiglione Catchment," *Hydrology and Earth System Sciences*, Vol. 24, pp. 5781–5798, 2020.

[38] Y. Alabbad, and I. Demir, "Urban Flood Impact Assessment and Hazard Vulnerability Analysis: Iowa Case Study," *Earth Arxiv*, Vol. 3051, pp. 1-26, 2022.

[39] O. Obroh, and G. Sambo, "Flood Vulnerability Mapping of River Ngadda Using Geospatial and Remote Sensing Techniques Maiduguri Metropolis, Borno State," *Journal of Global Ecology and Environment,* Vol. 14, Issue 4,

pp. 44-58, 2022.

[40] S. Fernandez, and A. Lutz, "Urban flood hazard zoning in Tucumán Province, Argentina, using GIS and multicriteria decision analysis," *Engineering Geology*, Vol. 111, Issue 1-4, pp. 90–98, 2010.

[41] C. Xu, Y. Chen, Y. Chen, R. Zhao, and H. Ding, "Responses of surface runoff to climate change and human activities in the arid region of Central Asia: A case study in the Tarim River Basin, China," *Environmental Management*, Vol. 51, pp. 926–938, 2013.

[42] K, Poussin, W. Botzen, and H. Aerts, "Factors of influence on flood damage mitigation behavior by households," *Environmental Science & Policy*, Vol. 40, pp. 69–77, 2014.

[43] W, Wang and Y, Lu, "Analysis of the Mean Absolute Error (MAE) and the Root Mean Square Error (RMSE) in Assessing Rounding Model," *IOP Conf. Series: Materials Science and Engineering*, Vol. 324, pp. 1-11, 2018.

[44] M. Alivio, R. Puno, and B. Talisay, "Flood hazard zones using 2d hydrodynamic modeling and remote sensing approaches," *Global Journal of Environmental Science and Management*, Vol. 5, no. 1, pp. 1-16, 2019.

[45] L. Hawker, P. Bates, J. Neal, and J. Rougier, "Perspectives on digital elevation model (DEM) simulation for flood modeling in the absence of a high-accuracy open access global DEM," *Frontiers in Earth Science*, Vol. 6, no. 233, pp. 1-9, 2018.

[46] A. Jothibasu, and S. Anbazhagan "Flood Susceptibility Appraisal in Ponnaiyar River Basin, India using Frequency Ratio (FR) and Shannon's Entropy (SE) Models," *International Journal of Advanced Remote Sensing and GIS*, Vol. 5, no. 10, pp. 1946-1962, 2016.

[47] M. Tehrany, L. Kumar, M. Jebur, and F. Shabani, "Evaluating the application of the statistical index method in flood susceptibility mapping and its comparison with frequency ratio and logistic regression methods," *Geomatics, Natural Hazards and Risk*, Vol. 10, no. 1, pp. 79–101, 2019.

[48] A. Jaafari, A. Najafi, H. Pourghasemi, J. Rezaeian, and A. Sattarian, "GIS-based frequency ratio and index of entropy models for landslide susceptibility assessment in the Caspian forest, northern Iran," *International Journal of Environmental Science and Technology*, Vol. 11, no. 4, pp. 909–926, 2014.

[49] M. Sahana, and P. Patel, "A comparison of frequency ratio and fuzzy logic models for flood susceptibility assessment of the lower Kosi River Basin in India," *Environmental Earth Sciences*, Vol. 78, no. 10, pp. 1-27, 2019.

[50] S. Kumari, and N. Goudar, "Flood Susceptibility Mapping using Frequency Ratio and Shannon's Entropy Models in the Plains of North Bihar, India," *Global Research and Development Journal*, Vol. 6, Issue 12, pp. 1-8, 2021.

[51] S. Maria, and Z. Martina, "Flood risk assessment and flood damage Evaluation – The Review of the Case Studies," *Acta Hydrologica Slovaca*, Vol. 22, no. 1, pp. 156 – 163, 2021.

[52] S. Singh, S. Kanga, B. Durin, N. Kanjcic, R. Chaurasia, and D. Markovinovic, "Flood risk modeling using HEC-RAS and geospatial techniques," *Electronic collection of papers of the Faculty of Civil Engineering*, Vol. 11, Issue 22, pp. 20-36, 2021.

[53] A. Salman, S. Hassan, G. Khan, M. Goheer, A. Jhan, and K. Sheraz, "HEC-RAS and GIS-based flood plain mapping: A case study of Narai Drain Peshawar," *Acta Geophysica*, Vol. 69, pp. 1383–1393, 2021.

[54] K. Chapi, V. Singh, A. Shirzadi, H. Shahabi, D. Bui, B. Pham, and K. Khosravi, "A novel hybrid artificial intelligence approach for flood susceptibility assessment," *Environmental Modelling & Software*, Vol. 95, pp. 229–245, 2017.

[55] W. Namara, T. Damisse, and F. Tufa, "Application of HEC-RAS and HEC-GeoRAS model for Flood Inundation Mapping, the case of Awash Bello Flood Plain, Upper Awash River Basin, Oromiya Regional State, Ethiopia," *Modeling Earth Systems and Environment*, Vol. 8, pp. 1-12, 2021.

[56] B. Merz, A. Thieken, and M. Gocht, "Flood risk mapping at the local scale: concepts and challenges," *Flood Risk Management in Europe*, Vol. 25, pp. 231–251, 2007